Stochastic time-series models for drought assessment in the Gaza Strip (Palestine)

Hassan Al-Najjar IWA, Gokmen Ceribasi, Emrah Dogan, Mazen Abualtayef, Khalid Qahman and Ahmed Shaqfa

ABSTRACT

The Eastern Mediterranean region of the Middle East and North Africa (MENA) is experiencing patterns of major drought due to the effects of rising temperatures and falling precipitation levels. The multiscale drought evaluation Standardized Precipitation Evapotranspiration Index (SPEI) reveals evolving and severe drought from North Africa and the Sinai desert toward the Middle East. While there has been a period without drought between 1970 and 1990, the severity and frequency of drought increased considerably after 1990. Current drought conditions in the Eastern Mediterranean region of MENA are moderate to severe with a 60–100% likelihood of occurrence, according to time parameters. The Gaza Strip is especially vulnerable to the consequences of increasing drought because it is situated in the vicinity of the Sinai Desert; therefore, a downscaled study of drought in the region is essential to implement mitigation measures for the sustainable management and planning of coastal aquifer and agricultural activities in the Gaza Strip. Considerable availability of precipitation time series from various meteorological stations helped provide a local drought study for the Gaza Strip, in accordance with the Standardized Precipitation Index (SPI). The stochastic time-series model of $(4,0,1)$ $(5,1,1)_{12}$ shows a robust simulator for modeling and forecasting the future trend of precipitation at the nine meteorological stations. In terms of correlation accuracy, the model achieves a correlation (r) of approximately 93–97% in the calibration range and a correlation (r) of about 92–99% in the validation range. In terms of measuring the difference between the values, the root mean squared error (RMSE) of the model results shows that the RMSE was between 7–21 in the calibration range and 11–21 in the validation range. The model reveals a slightly stable trend in precipitation patterns at the northern meteorological stations of Beit Hanon, Beit Lahia, Shati, and Remal. However, declining precipitation tendency was recorded at the southern meteorological stations of Mughraka, Nussirat, Beir Al-Balah, Khanyounis, and Rafah. The SPI-based drought assessment implies that the precipitation annual threshold levels at $SPI = 0$ drop territorially from 474 mm in the north to about 250 mm in the south of the Gaza Strip. In this study, a representative 12-month local scale SPI_{12} at an annual precipitation threshold level of 370 mm was formulated to address the drought conditions in the Gaza Strip. Standing on the outputs of the local SPI_{12} scale might signify that the region of the Gaza Strip risks drought status with an incidence likelihood varying from 8% in the north to 100% in the south. Regular drought is prevalent in the northern governorates, but the hazards of extreme and severe drought are high in the southern areas with an incidence risk of about 83%. Sequentially, southern governorates of Rafah and Khanyounis experience chronic annual drought, while the return period of drought is reported to be every 9–12 years in the northern governorates of the Gaza Strip. The rain-fed years of 1998 and 2010 reported the worst periods of drought, while the period of 2016 showed a good droughtless water balance. Overall, the no-drought status might define the prospective conditions in the governorates of North

Hassan Al-Najjar IWA (corresponding author)
Department of Civil Engineering, Institute of
  Natural Sciences,
Sakarya University,
54187 Sakarya,
Turkey
E-mail: hassan.al-najjar@ogr.sakarya.edu.tr

Gokmen Ceribasi
Department of Civil Engineering, Technology
  Faculty,
Sakarya University of Applied Sciences,
54187 Sakarya,
Turkey

Emrah Dogan
Department of Civil Engineering, Faculty of
  Engineering,
Sakarya University,
54187 Sakarya,
Turkey

Mazen Abualtayef
Ahmed Shaqfa
Department of Civil and Environmental
  Engineering,
Islamic University of Gaza,
Gaza,
Palestine

Khalid Qahman
Environment Quality Authority,
Gaza,
Palestine

Gaza, Gaza, and central Gaza over the next 20 years, while Rafah and Khanyounis are anticipated to be under normal to severe drought conditions.

Key words │ ARIMA, drought, forecasting, stochastic, Gaza Strip, time series

HIGHLIGHTS

- The drought is significantly demonstrated by the SPEI in the MENA.
- The stochastic models show high accuracy in forecasting.
- The Gaza Strip experiences intensity in drought occurrence.

INTRODUCTION

Climatic drought is a phenomenal evidential sign of climate change that affects the natural conditions of water resources (Dai *et al.* 2004; IPCC 2007; Sheffield & Wood 2011; Intergovernmental Panel on Climate Change (IPCC) 2014; Sheffield *et al.* 2014). Globally, drought is being reported as the most extensive natural hazard that occurs in arid and semi-arid regions, which can cause stark economic, social, and environmental damage (Nagarajan 2010; Mondol *et al.* 2017). Evidentially, droughts of greater severity are expected more frequently, for longer, and to cover a broader area due to global warming, which causes greater disruption (Han & Singh 2020). Agricultural production is among the most vulnerable sectors to drought where one instance could reduce global agricultural productivity by 0.8% and around three-quarters of globally cultivated areas experience periodic losses from drought estimated at approximately 6–7 billion USD per year (Kim *et al.* 2019). The losses caused by drought are projected to increase dramatically due to potential increases in the incidence of drought in the future. A commonly reported fact is that a 1 °C increase in temperature is strongly linked to a 1.4% decrease in annual income (Dell *et al.* 2012). In 1975, the drought-related crop losses in the Great Plains of the United States were estimated to be worth 700 million USD (White & Haas 1975). However, annual losses from drought in the United States amount to an estimated 6–8 billion USD (FEMA 1995). The prolonged drought of California triggered crop losses worth nearly 5.5 billion USD in the years 2011–2017, and the forests lost more than 130 million types of plants (Kam *et al.* 2019). The Millennium drought reported between 1997 and 2009 was one of the worst droughts of below-average precipitation in Southeast Australia, which severely impacted the ecosystem and economy (CSIRO 2012; Leblanc *et al.* 2012; AghaKouchak *et al.* 2014; Xie *et al.* 2016). In response to the drought, integrated national and state institutional frameworks in parallel with water conservation programs like water recycling and seawater desalination were adopted to alleviate the consequences of future drought variabilities (Low *et al.* 2015). Banerjee *et al.* (2013) estimated that the economic costs of handling the disruption in the hydrological environment in South Australia during the Millennium drought to be approximately 810 million USD. The projections of the local economy reveal that the consequences of drought lead to a decrease of around 1–2% in Australia's national gross domestic product (GDP) per year (Haque *et al.* 2017). In this context, the African Sahel region demonstrates an extreme example of multi-decadal climate variability that has occurred since the 1960s due to the sharp decrease in the rainfall patterns. From the 1950s until the present day, the temperature has risen to 3.5 °C in the Sahel region, and this increases the evaporation process from the soil and water surfaces and negatively affects the water security and food production for about 100 inhabitants in this area (van der Geest *et al.* 2019). Principally, the classification of droughts relates to the decreases in the climatological factor of precipitation to a level less than normal over a geographical area that subsequently impacts the natural sustainability of the hydrological systems (Shukla & Wood 2008; Mishra & Singh 2010; Efstathiou & Varotsos 2012; Keka *et al.* 2012; Almedeij 2014; Shah *et al.*

2015). The drought is identified as a slowly evolving phenomenon that has an elliptical profile in the temporal and spatial propagation (Shahid & Behrawan 2008; Al-Qinna *et al.* 2010; Patterson *et al.* 2013; Shah *et al.* 2015). Therefore, the assessment of the drought severity, spatial and temporal dispersion, and the frequency of occurrence is a prerequisite for an integrated water resource, economic and agricultural management, and planning system (Mishra & Singh 2010; Kampragou *et al.* 2011; Moreira *et al.* 2015; Nam *et al.* 2015; Kwak *et al.* 2016; Alqaysi *et al.* 2017; Awchi & Kalyana 2017; Mehr *et al.* 2019; Baruga *et al.* 2020). Many drought investigations in the regions of the Middle East and North Africa (MENA) indicate that these regions face chronic consequences from drought, strains on the integrity of water resources, and increases in the impact of the water crisis (Sönmez *et al.* 2005; Abbaspour *et al.* 2009; Al-Qinna *et al.* 2010; Keramat *et al.* 2011; Sen et al. 2012; Kelley *et al.* 2015; Modarres *et al.* 2016; Awchi & Kalyana 2017; Habibi *et al.* 2018; Aladaileh *et al.* 2019). Decision-making requires a rigorous preventive drought mitigation strategy, dependent on accurate drought monitoring and forecasting that is based on defining drought contingencies in the context of oceanic atmospheric-land dynamics and hydrological conditions (Hao *et al.* 2018). Accordingly, multiple statistical, dynamic, and hybrid model simulations have been developed for drought forecasting. The dynamic drought forecasting models are future climate projections of the ocean–atmosphere–land processes based on coupling the general circulation models of climate. However, statistical forecasting approaches simulate the future climate by utilizing the previously observed values (Yuan & Wood 2013; Saha *et al.* 2014). The statistical models exhibit greater accuracy in addressing local drought behaviors than dynamic models that are more appropriate for large-scale studies. However, the limitations of statistical models in detecting the nonstationary nature of climate systems, and the weakness of dynamical models in long-term predictions due to the random nature of the ocean–atmosphere circulation, make the hybrid statistical–dynamic simulation approaches a preferable option to forecast the climatic phenomena (Mishra & Singh 2010; Madadgar *et al.* 2016; Hao *et al.* 2018; Xu *et al.* 2018; Strazzo *et al.* 2019; Han & Singh 2020). Nevertheless, the variety and the simplicity of the statistical forecasting models conceptual structures of machine learning (Kuswanto & Naufal 2019; Zhang *et al.* 2019; Khan *et al.* 2020), time-series models (Moghimi *et al.* 2019; Yeh & Hsu 2019), probability models (Paredes & Guevara 2013; Behrangi *et al.* 2015; Avilés *et al.* 2016; Hao *et al.* 2016; Jouybari-Moghaddam *et al.* 2017), regression models (Stagge *et al.* 2015; Mortensen *et al.* 2018), and hybridized models (Rezaeianzadeh *et al.* 2016; Prasad *et al.* 2018; Fung *et al.* 2019; Malik *et al.* 2020) reinforce the trend to rely on these approaches for establishing regional and local analytical drought studies (Anshuka *et al.* 2019). As aforementioned, the science and the historical data provide the basis for developing descriptive drought models. Hence, the aggregation of the prior distribution of observations conveys the predictive information about the immediate future (Nagarajan 2010). Therefore, the stochastic approaches utilize the power of stochastic models such as Autoregressive Integrated Moving Average (ARIMA) or Markov Chain to simulate the temporal propagation of drought (Cancelliere & Salas 2004; Mishra & Desai 2005; Modarres 2007; Serfozo 2009; Han *et al.* 2010). Similarly, the statistical approach employs various statistical techniques to estimate drought characteristics, and these techniques can also mainly be divided into statistical modeling and probabilistic distribution (Cancelliere *et al.* 2007; Kwak *et al.* 2016). Specifically, drought analytical studies are fundamentally based on the stochastic statistics of drought indices (Munger 1916; Cancelliere *et al.* 2007; Kwak *et al.* 2016). The index approaches are based on computing a unique value of drought in terms of different meteorological inputs, such as precipitation, evaporation, and transpiration, to classify the severity and the frequency of drought (Palmer 1965; Gibbs & Maher 1967; Palmer 1968; Shafer & Dezman 1982; Petrasovits 1990; McKee *et al.* 1993; Sastri 1993; Kogan 1995; Guttman 1998; Byun & Wilhite 1999; Szalai & Szinell 2000; Samkhtin and Hughes 2004; Morid *et al.* 2006; Tsakiris *et al.* 2007; Vicente-Serrano *et al.* 2010; Hao & AghaKouchak 2013; Wichitarapongsakun *et al.* 2016; WMO & GWP 2016). The Standardized Precipitation Index (SPI) is the most popular meteorological drought index used to assess the expected drought due to the change in the precipitation behavior over different periods (McKee *et al.* 1985, 1993, 1995). The SPI introduces a comprehensive multi time-scaled assessment methodology for the effect of precipitation deficit on water resources in comparison

with the other indices (Manatsa *et al.* 2010; Du *et al.* 2013; Alqaysi *et al.* 2017; Halwatura *et al.* 2017). However, taking the influence of other climatic parameters, the Standardized Precipitation Evapotranspiration Index (SPEI) is considered a more reliable index to assess the impact of drought (Homdee *et al.* 2016; Tefera *et al.* 2019; Zhang *et al.* 2020). The spatial mapping of drought is necessary for policy-makers to understand the regional characteristics of drought to manage it effectively, to reduce agricultural production losses, and to protect the environment (Alamgir *et al.* 2015; Karavitis *et al.* 2015; Mondol *et al.* 2017; Uddin *et al.* 2020). In general, this study aims to assess the fluctuation in the temporal and spatial distribution of drought in the MENA. Moreover, a microstudy of the Gaza Strip in Palestine was implemented by developing forecasting stochastic time-series models and detecting the statistical features of drought occurrence throughout the period and the area of the study. The study sought to overcome the dearth in available studies on drought in the Eastern Mediterranean countries of MENA as well as the challenge of a lack of and missing meteorological data for drought investigations in the Gaza Strip by expanding stochastic models for simulating missing data and forecasting the meteorological state in the Gaza Strip.

DATA GENERATION AND TIMES SERIES ANALYSIS

The premise that history provides clues to the future is the foundation of forecasting. In hydrological and meteorological cases, the available observed data represent a general indication about past conditions, so forecasting seeks to extend the available data to examine how a particular sequence of data is likely to behave in the future (Werick & Whipple 1994; Issar 2003; Sene 2009; Hingray *et al.* 2014; Sharma *et al.* 2019). Data generation techniques and forecasting are essential for investigating risk factors, particularly those associated with flooding or drought (Gaur *et al.* 2018; Doroszkiewicz *et al.* 2019; Markus *et al.* 2019). The exact pattern shown in historical records is unlikely to be repeated in the future; however, the information in the available data could be used for probability distributions, statistical parameters, and in the use of general stochastic behavior to generate several sequences of data to

characterize the future. Therefore, the main principle behind the generation of data is to extract the significant statistical regularities or perturbs that could be found in the hydrological and meteorological series and that are more likely to occur in nature (Machiwal & Jha 2012). The data generation models are utilized to reproduce data that has the same mean, standard deviation, and correlation coefficient as the historical mean, standard deviation, and correlation coefficient, more or less. Therefore, the models are developed so that certain parameters or certain moments of the historical data are preserved in the generated sequence (Gupta *et al.* 2014; Hauser *et al.* 2017). The time series is a structure of random variable sequences collected over time like stream flows, rainfall, and temperature. The dependency of one value on another in the time series is the main basis for time-series analysis, generation of data, and forecasting. Accordingly, the synthetically generated data are valuable extractions from the past to simulate the prospective behavior of a specific system. The mathematical model, summarized in Equation (1), that represents the time series consists of a deterministic component, in addition to a stochastic random component to address certain random fluctuations of a process occurring around the deterministic component (Sharma *et al.* 2019).

$$x_t = d_t + \varepsilon_t \tag{1}$$

where x_t is a stochastic model; d_t is a deterministic component; ε_t is a stochastic random component.

The stochastic component is the dominant term in representing models while the existence of the deterministic component is not dominant (Machiwal & Jha 2012). The deterministic component is a combination of long-term mean, trend, periodicity, and jump (Kottegoda 1980). Generally, the time-series model is built by capturing the deterministic component and by simulating the behavior of the stochastic random component (Chatfield 2003).

The autocorrelation functions

The autocorrelation function (ACF), which is represented by a correlogram, represents the memory of the stochastic process and gives inherent information about how far in time

the process can remember what has happened before. The autocorrelation between x_t and x_{t+k} is addressed by Equation (2) as follows (Kashyap & Rao 1976; Chatfield 2003; Box *et al.* 2008):

$$\rho_k = \frac{\text{cov}\ (x_t, x_{t+k})}{\sigma_{x_t} . \sigma_{x_{t+k}}} \tag{2}$$

where ρ_k is the autocorrelation value; cov (x_t, x_{t+k}) the auto-covariance; x_t the original time series; $x_{t+k:}$ the timer series of lag k; σ_{xt} the variance of the original time series at lag zero; $\sigma_{xt+k:}$ the variance of time series at lag k.

Generally, to ensure purely stochastic random time series, the autocorrelation values for all lags except zero-lag autocorrelation should be statistically insignificant. The degree of dependency of any value on another value in the time series should also be addressed by partial ACF (PACF) analysis. The hypothesis that the time series follows the normal distribution is used to examine whether the sample time series comes from a purely stochastic series or not (Box & Jenkins 1970; Kashyap & Rao 1976).

Frequency domain analysis

The spectral analysis is widely used in the application of drought and flooding periodic analysis, generation of synthetic data, hydrologic forecasting, and climate change impact studies (Zhang *et al.* 2008; Kumbuyo *et al.* 2014). The ACF or correlogram is used for analyzing the time series in the time domain, which gives a general indication about inherent periodicities in the data. However, the exact and the significant periodicities in the data can be determined by analyzing the time series in the frequency domain or spectral analysis instead of the time domain (Kashyap & Rao 1976). The observed time series is considered as a random sample of a process over time and is made up of oscillations of all possible frequencies. The spectral analysis defines the time series as a combination of cosine and sine waves, as shown in Equation (3), as well as a random component (Koopmans 1974; Kashyap & Rao 1976; Kottegoda 1980).

$$x_t = a_o + \sum_{k=1}^{\frac{n-1}{2},\frac{n}{2}} [a_k \cos\ (2\pi f_k t) + \beta_k \sin\ (2\pi f_k t)] + \varepsilon_t \tag{3}$$

where a_o is the arithmetic mean of the time series; N is the number of time series observations; M is the maximum lag typically considered up to 0.25 N.

$$f_k = \frac{k}{N}$$

$$a_k = \frac{2}{N} \sum_{t=1}^{N} x_t \cos\ (2\pi f_k t) \qquad k = 1, 2, \ldots M$$

$$\beta_k = \frac{2}{N} \sum_{t=1}^{N} x_t \sin\ (2\pi f_k t) \qquad k = 1, 2, \ldots M$$

The variance spectrum divides that variance into several intervals or bands of frequencies. The spectral density (I_k) is the amount of variance per interval of frequency as described in Equations (4) and (5) (Kashyap & Rao 1976).

$$I_k = \frac{N}{2} \sum_{t=1}^{N} (\alpha_k^2 + \beta_k^2) \quad k = 1, 2, \ldots M \tag{4}$$

$$\omega_k = \frac{2\pi k}{N} = \frac{2\pi}{P} \quad k = 1, 2, \ldots M \tag{5}$$

where I_k is the spectral density; ω_k is the angular frequency; P is the periodicity; k is the lag.

Remarkably, the total area under the spectrum is equivalent to the variance of the process. A significant peak in the spectrum indicates an important contribution to variance at frequencies close to the peak; prominent spikes indicate significant periodicity. The spectral density or the line spectrum transforms the information from the time domain to the frequency domain. Hence, while the correlogram indicates the presence of periodicities in the data, the spectral analysis identifies the significance of periodicities themselves. The line spectrum is an inconsistent estimate and is not a smooth function. The power spectrum is the smoothened version of the spectrum and it demonstrates the consistent estimate of the spectral density. The Fourier cosine transform power spectrum, shown in Equation (6), is a common type for frequency analysis (Kashyap & Rao 1976):

$$I_k = 2 \left[c_o + 2 \sum_{j=1}^{\frac{N-1}{2}} \lambda_j c_j \cos\ (2\pi f_k j) \right] \tag{6}$$

where c_j is auto-covariance function; λ_j lag window or smoothing window.

A well-known form, depicted in Equation (7), which is widely used to formulate the lag window, is the Tukey's window (Kashyap & Rao 1976).

$$\lambda_j = \frac{1}{2}\left[1 + 2\cos\left(\frac{2\pi}{M}\right)\right] \tag{7}$$

The spectrum shows prominent spikes that represent the periodicities inherent in the data. In the case of a completely random time series that has uniformly distributed random values, the spectral density function is constant and termed as white noise. The white noise indicates that there is no significant frequency interval containing variance more than the frequency interval of zero-lag. Statistically, the significance of the periodicity (k) is tested using the F-test at a specific significance level (α) by defining a statistic ($\bigcap$) as described in Equation (8) (Kashyap & Rao 1976):

$$\bigcap = \frac{\gamma_k^2\,(N-2)}{4\hat{\rho}_1} \tag{8}$$

where

$$\gamma_k^2 = \alpha_k^2 + \beta_k^2$$
$$\hat{\rho}_1 = \frac{1}{N}\left[\sum_{t=1}^{N}\{x_t - \hat{\alpha}_k\cos(\omega_k t) - \hat{\beta}_k\sin(\omega_k t)\}\right]$$

Principally, a necessary condition in the stochastic models is that the series being modeled must be free from any significant periodicities. Thus, for periodicity to be removed from the time series, the original time series is simply transformed into another pure one by differencing or by standardization method (Box & Jenkins 1970; Kashyap & Rao 1976).

Autoregressive Integrated Moving Average (ARIMA) models

Time-series models are built by analyzing the past to predict the future by forecasting, to provide a proper perspective view for the managers and policymakers to make well-informed and sound decisions. An important feature of most time series is that the observations are serially dependent. In general, the time series can be decomposed into four components: a secular trend, seasonal variation, cyclical variation, and irregular variation that can be modeled deterministically with mathematical functions of time (Kottegoda 1980; Sharma *et al.* 2019). The ARIMA models are types of Box Jenkins models that stand on the concept of autoregression by regressing, mathematically described in Equation (9), a single variable upon itself at different periods (Box & Jenkins 1976; Tong 1990; Polyak 1996).

$$x_t = f(x_{t-1}, x_{t-2}, x_{t-3}, \cdots) \tag{9}$$

In general, the mathematical terms shown in Equation (10) demonstrate the comprehensive form of the ARIMA model, which is written in the following form (Shahin *et al.* 1993):

$$\left[1 - \sum_{i=1}^{p}\varnothing_i B^i\right]\cdot\left[1 - \sum_{i=1}^{P}\varnothing_{is}B^{i\times s}\right]\cdot(1-B)^d\cdot(1-B^s)^D x_t$$
$$= \left[1 + \sum_{i=1}^{q}\theta_i B^i\right]\cdot\left[1 + \sum_{i=1}^{Q}\theta_{is}B^{i\times s}\right]\cdot\varepsilon_t \tag{10}$$

where ϕ_i is the ith autoregressive (AR) parameters; Φ_{is} the ith seasonal autoregressive (AR) parameters; θ_i the ith moving average (MA) parameters; θ_{is} the ith seasonal moving average (MA) parameters; B the backshift operator; d the differencing; D the seasonal differencing; S the seasonality period; ε_t a noise random component.

The stochastic ARIMA models are widely used in water resource management applications, especially for modeling hydrological stream flows, groundwater level fluctuations, and drought patterns (Bazrafshan *et al.* 2015; Mirzavand & Ghazavi 2015; Djerbouai & Souag-Gamane 2016; Khorasani *et al.* 2016; Myronidis *et al.* 2018; Takafuji *et al.* 2018; Sakizadeh *et al.* 2019).

THE SPI AND THE SPEI

The SPI is a multiple time scale that is used for precipitation conditions and water supply evaluation. The SPI values present the standard deviation of the normalized precipitation values from the mean, which enables the assessment of dry and wet periods (McKee *et al.* 1993). Mathematically,

the function described in Equation (11) highlights the gamma distribution function for fitting the monthly precipitation series (Thom 1958).

$$f(x) = \frac{1}{\beta^\alpha \Gamma(\alpha)} x^{\alpha-1} e^{-x/\beta}, \quad x > 0 \tag{11}$$

Then, the resulting parameters are used to estimate the cumulative probability of historical precipitation. However, to take into consideration the contained zero-precipitation values in the time series, the gamma cumulative distribution function (CDF) is being modified into a more generalized CDF as shown in the following equation:

$$F(x) = u + (1 - u) \times \int_0^x f(x)dx \tag{12}$$

The modified CDF is introduced into a standard normal distribution, as shown in the below equation, following the described numerical method by Abramowitz & Stegun (1970).

$$\text{SPI} = Z =$$
$$\begin{cases} -\left(k - \dfrac{2.516 + 0.803k + 0.010k^2}{1 + 1.433k + 0.189k^2 + 0.001k^3} \right) & \text{if } 0 < F(x) \leq 0.5 \\ +\left(k - \dfrac{2.5156 + 0.803k + 0.010k^2}{1 + 1.433k + 0.189k^2 + 0.001k^3} \right) & \text{if } 0.5 < F(x) \leq 1 \end{cases}$$
$$\tag{13}$$

$$k = \begin{cases} \sqrt{\ln\left[1/(F(x))^2\right]} & \text{if } 0 < F(x) < 0.5 \\ \sqrt{\ln\left[1/1 - (F(x))^2\right]} & \text{if } 0.5 < F(x) < 1 \end{cases}$$

where $f(x)$ is the gamma distribution function; $F(x)$ is the modified gamma distribution function; A and β are the shape and scale parameters, respectively; X is the precipitation amount; $\Gamma(\alpha)$ is the gamma function; and u is the probability of zero precipitation.

The SPEI is a nonexceedance probability value computed on the difference between the precipitation and the potential evapotranspiration (PET) as shown in the following equation (Tirivarombo et al. 2018):

$$\text{SPEI} = W - \frac{2.516 + 0.803W + 0.01W^2}{1 + 1.433W + 0.189W^2 + 0.001W^3} \tag{14}$$

where $W = \sqrt{-2\ln(P)}$ for $P \leq 0.5$.

P is the probability of exceeding a determined D_i value and is given as $P = 1 - f(x)$, where

$$D_n^k = \sum_{i-0}^{k-1} P_{n-1} - (\text{PET})_{n-1}$$

The probability density function of a Log-logistic distribution is given as shown in the following equation:

$$f(x) = \frac{\beta}{\alpha} \cdot \left(\frac{x-y}{\alpha}\right)^{\beta-1} \left(1 + \left(\frac{x-y}{\alpha}\right)^\beta\right)^{-2} \tag{15}$$

Accordingly, as demonstrated in Table 1, the computed SPI and SPEI values are used to classify the severity of drought that has occurred, based on four designated drought categories by McKee et al. (1993).

The advantages of SPI and SPEI are due to its considerable ability to quantify the precipitation deficit for several time scales to address the consequential impacts of agricultural drought, hydrological drought, and groundwater drought (Bazrafshan 2007; Elkollaly et al. 2017; Javanmard et al. 2017; Caloiero et al. 2018; Abeysingha & Rajapaksha 2020). Hence, the recharge of the groundwater is evaluated every 12 months. The SPI period of 12 months is the commonly recommended time scale to address the impact of annual drought behavior on the groundwater balance.

Table 1 | Drought categories (McKee et al. 1993)

SPI values	Drought category
− 2.00 and less	Extreme drought
− 1.50 to −1.99	Severe drought
− 1.00 to −1.49	Moderate drought
− 0.99 to 0	Normal drought
More than 0	No drought

DROUGHT IN THE EASTERN MEDITERRANEAN REGION OF THE MENA

Throughout this study, the MENA countries that lie on the eastern coast of the Mediterranean Sea, shown in Figure 1, were highlighted to describe the nature of the regional drought. The study area covers about 1.3 million km², where around 180 million people reside. The drought noticeably increases in this area, especially in Egypt, which has a negative effect on agricultural production and food security (Hameed *et al.* 2020). Prolonged droughts are inherently part of the natural climate of the area where there is a substantial decrease in precipitation in tandem with temperature rises in the area (Elasha 2010; IPCC 2014). The Middle East area is known to be the driest area in the world, and historical measurements reveal extreme and alternating periods of drought in the region (Kelley *et al.* 2015; Sharifi *et al.* 2015; Huang *et al.* 2016). The Mediterranean region of the Middle East shows more decline in precipitation trends than other areas, which leads to a more prolonged drought in the coastal region of MENA (Karami 2016). The coastal strip of North Africa faces continual drought warnings due to the effect of the Sahel Desert region (Elasha 2010). Additionally, the Eastern Mediterranean region is under intense and increasing drought conditions that have been recorded since 1998 as observations and model simulations have shown how the number of warm events have doubled since the 1970s (Cook *et al.* 2016; Lelieveld *et al.* 2016). Moreover, the drought is more likely to occur in the arid and semi-arid areas of MENA where the climate experiences losses in the effective moisture over the region, which is increasing in aridity (El Kenawy *et al.* 2016). In general, the prolonged drought in the MENA is attributed to anthropogenic and nonanthropogenic components; however, the nonanthropogenic components can be considered a more reliable explanation for the drought in the MENA (IPCC 2014). Principally, the interaction between precipitation and evaporation processes is the main driver for drought pattern formation and this is basically related to many climatic processes in the region such as El Niño-Southern Oscillation, Southern Annular Mode, Indian Ocean Dipole, and North

Atlantic Oscillation (Golmohammadian & Pishvaei 2014). Noticeably, in the last 20 years, the region of MENA faces tangible losses due to drought, where considerable large agricultural areas were lost – around 50% of the irrigated land and 80% of the rain-fed cultivated land were absolutely lost (Huttner 2014).

To characterize the drought evolution in the Eastern Mediterranean region of MENA, the SPEI that is given by the Global SPEI database (https://spei.csic.es) was gathered, screened, and presented regionally. The Global SPEI database offers long-term, robust information about drought conditions on the global scale, with a $0.25 \times 0.25°$ spatial resolution cell and a monthly time resolution. It has a multiscale character, providing SPEI time scales between 1 and 48 months. The average SPEI for the area of study was presented based on 3-, 6-, 9-, and 12-month time scales, shown in Figure 2, for the period from 1970 until 2019. According to the data presented, the 1970–1990 period was in a state of no drought. However, after 1990, climatic conditions become drier. Remarkably, the drought's origins could be geographically pinpointed to the region of North Eastern Egypt and specifically, the Sinai Peninsula. According to categories from McKee *et al.* (1993), the drought in the area can be classified as being between normal and severe. The southern part of the Eastern Mediterranean region of MENA is currently under severe drought conditions, which negatively affects the integrity of water resources and other environmental components.

In terms of the drought occurrence, the projections significantly reveal an increasing trend in the incidence of drought as shown in Figure 3. Marginally, drought probability increases from less than 20% during the 1970s to more than 80% in the period 2010–2019.

In the Gaza Strip area, the drought became a recorded phenomenon that affected the recharge of the coastal aquifer and the sustainability of life. The drought conditions of 2007–2008, where the total rainfall amounted to 67% of the area's annual average, caused a direct loss in agricultural output and 114 million USD and around 200,000 types of livestock were affected (MoA 2008). As the previous figures show, the area of the Gaza Strip is experiencing drought that is increasing in severity and its probability of occurrence is
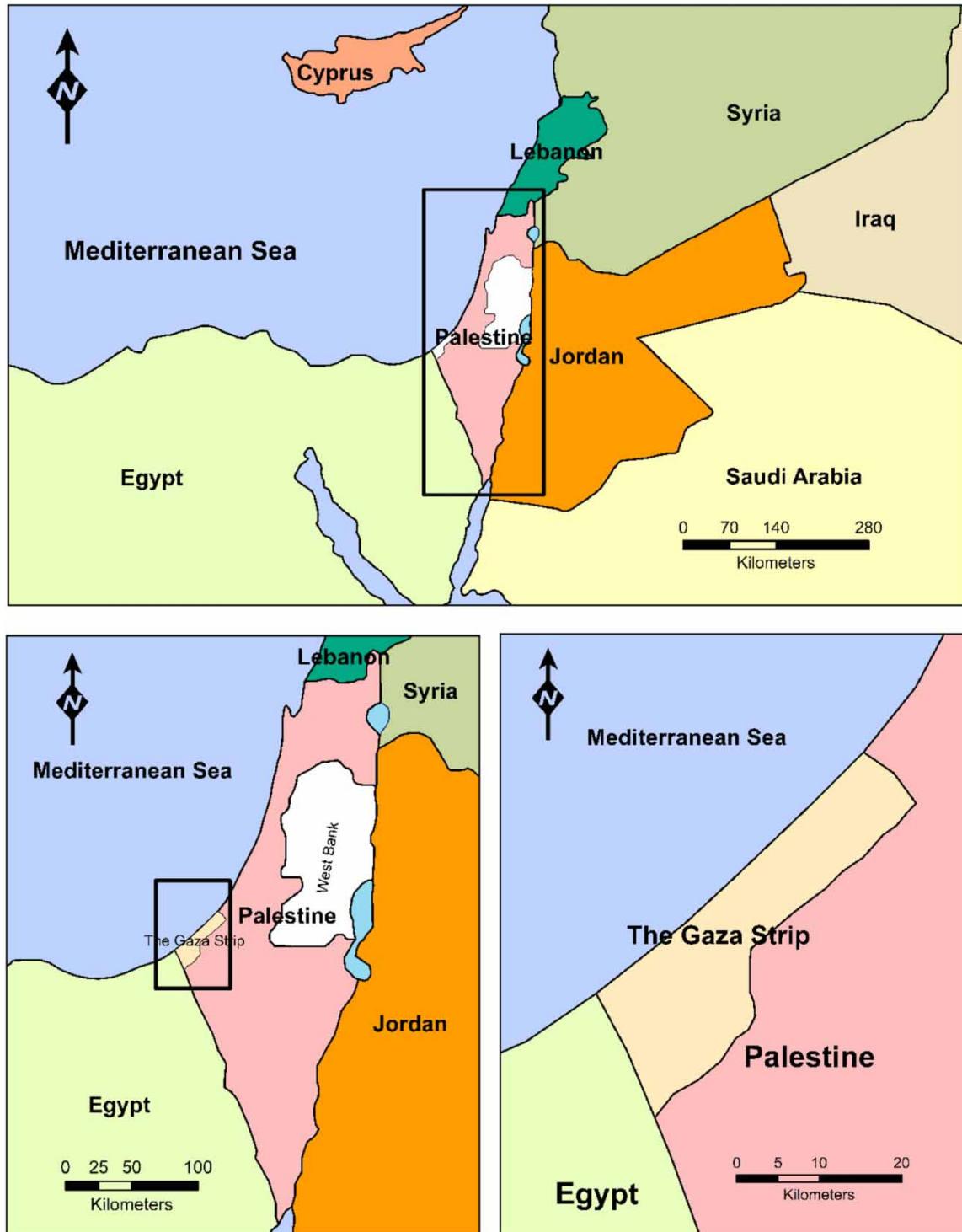
Figure 1 | The geographical location of Eastern Mediterranean countries of MENA and the location of the Gaza Strip.

approximately 60–80% every 3 months, and more than 80% every year. The aridity index in the Gaza Strip ranges between 0.16 and 0.3 and is expected to decrease due to the effect of climate change, decreases in precipitation, and increases in the temperature. From an economic perspective, 4.7% of the labor force is employed in the
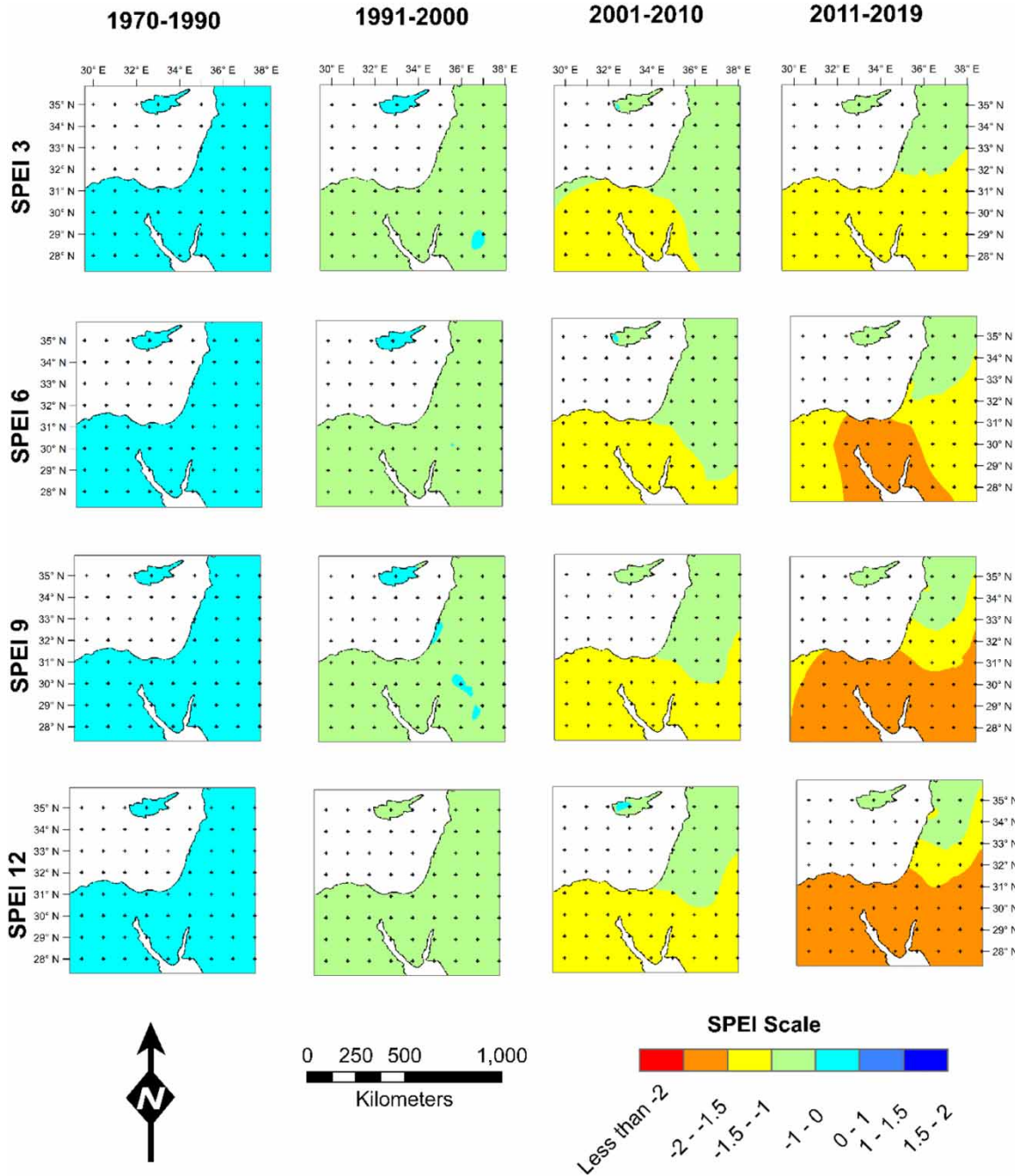
Figure 2 │ SPEI drought index for the Eastern Mediterranean of MENA for the period between 1970 and 2019.

agricultural sector and around 10% in fishing. The unemployment rate is around 41% and as a result of drought intensity, it is expected that more of the labor force will lose their jobs, particularly in the agricultural sector (PCBS 2020).

OVERVIEW OF THE GAZA STRIP (PALESTINE)

The Gaza Strip (Figure 4(a)) is a coastal stretch of land that extends on the southeastern coast of the Mediterranean Sea around 42 km long, between 6 and 12 km wide, and
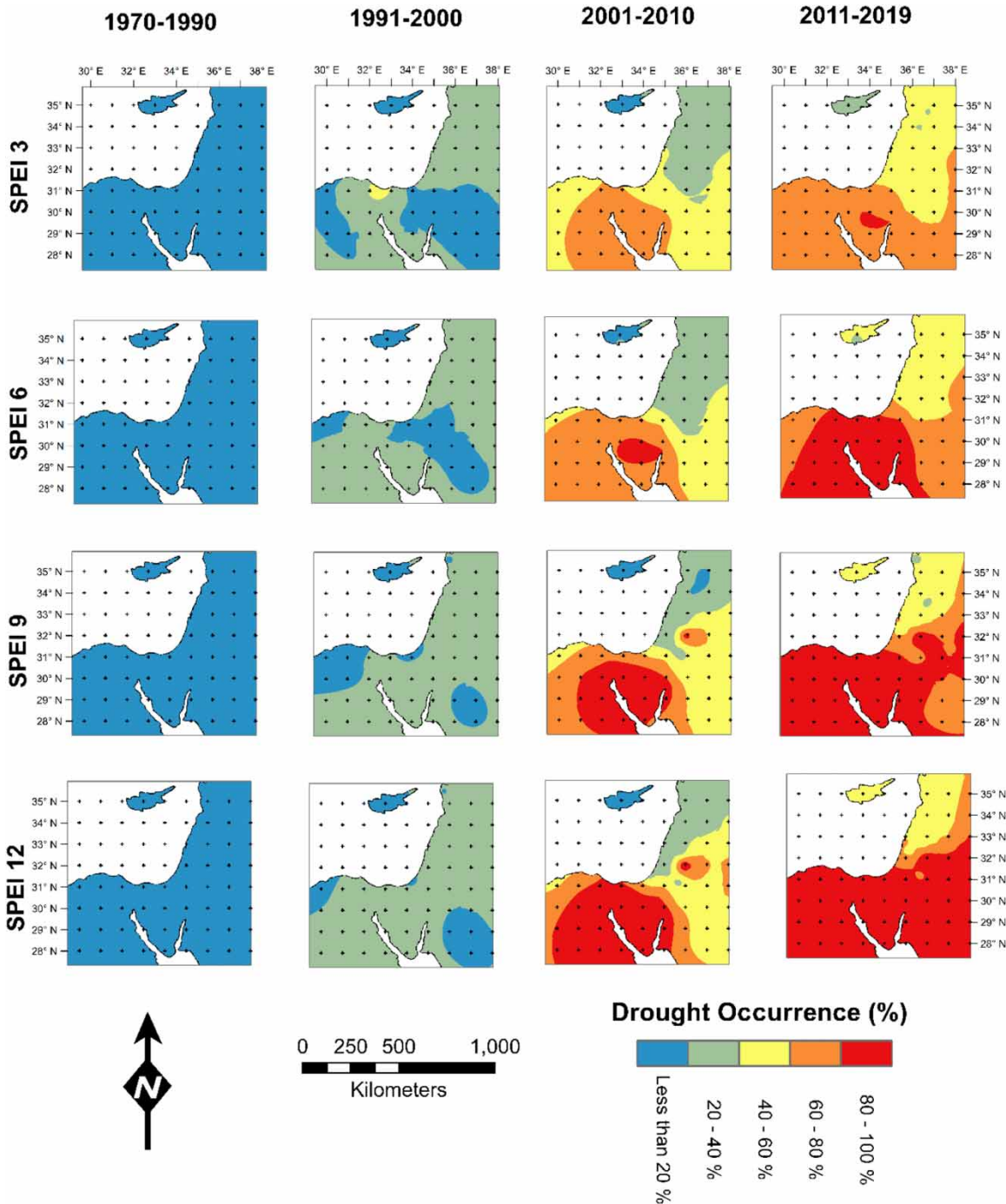
Figure 3 │ Drought occurrence in the Eastern Mediterranean of MENA.

which covers an area of 365 km^2. The Gaza Strip is characterized as being one of the most densely populated areas in the world. Therefore, according to the estimations of the Palestinian Central Bureau of Statistics (PCBS) for the year of 2019, the population of the Gaza Strip was 1.99 million inhabitants and the statistical projections show that the population will reach approximately 2.11 million inhabitants by 2021 (PCBS 2020). Geographically, the
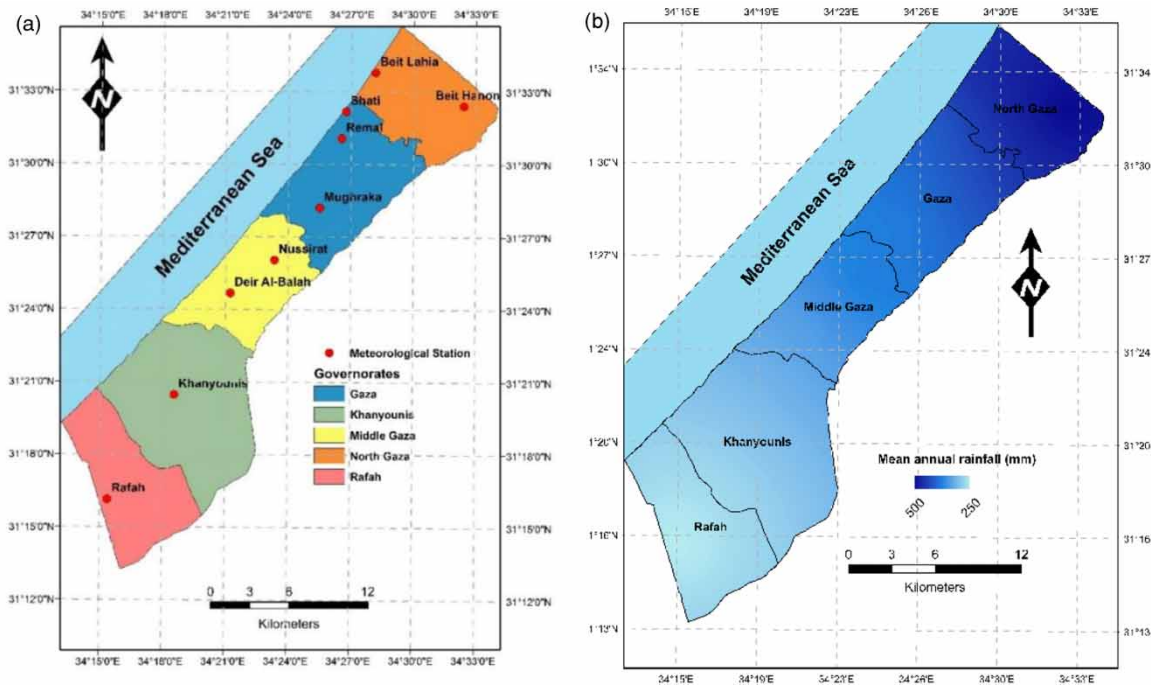
Figure 4 | The map of the Gaza Strip: (a) meteorological stations and (b) rainfall distribution.

climate of the Gaza Strip is generated by the interaction between the climates of the arid desert of the Sinai Peninsula and the semi-humid Mediterranean. In the Gaza Strip, the mean monthly temperature varies from 29 in summer to 10 in winter. The rainy months arrive in tandem with the winter season from October to March and as shown in Figure 4(b), the total annual rainfall in the area varies between around 470 mm in the north and 250 mm in the south of the Gaza Strip. In winter and summer, respectively, the actual monthly evaporation process is 95 and 185 mm, the monthly relative humidity fluctuates between 68 and 75%, and the mean duration of sunshine is between 190 and 305 h. The sea breeze blows in throughout the day and the land breeze blows during the night in the summer at an average regular velocity of about 8–9 mph, primarily from the northwest direction. At midday, the wind speed hits its peak intensity and declines until sunset. The storms are widely reported in the winter with a wind speed of up to 40–50 mph and, in normal conditions, the wind blows from the southwest at an average speed of 10 mph.

Concerning issues regarding water, existing conditions in the Gaza Strip are described as undergoing a severe water crisis. The coastal aquifer is the only available water resource for water supplies in the Gaza Strip. Nonetheless, owing to low recharge levels and the excessive abstraction from water wells, the coastal aquifer is being continuously depleted. The Gaza coastal aquifer monitoring program indicates that more than 95% of groundwater is unacceptably polluted (Palestinian Water Authority (PWA) 2014). Driven by the effect of seawater intrusion, chloride concentration is found to a considerable degree in groundwater, which exceeds the World Health Organization (WHO) chloride level (Qahman & Larabi 2006; Zaineldeen et al. 2013; Dentoni et al. 2014; El Baba et al. 2020). The annual water obtained from the coastal aquifer via the metered water wells amounts to around 200 million cubic meters, which is approximately four times the volume that the aquifer can recover sustainably per year (PWA 2011, 2012, 2013, 2014, 2015; Abualtayef et al. 2017; Mushtaha & Walraevens 2018). Agricultural lands comprise approximately 33% of the total land of the Gaza Strip and require around 90 million cubic meters of water annually, which is largely obtained from groundwater wells (PWA 2013; Ministry of Agriculture (MoA) 2016). Like other Eastern Mediterranean countries, the region of the Gaza Strip is experiencing a rise in extreme

drought events due to the influence of climate change on the rainy seasons, which significantly raises the vulnerability of food and water resources (Gampe *et al.* 2016; FAO 2018). Relatedly, Palestinian governmental institutions have adopted sustainable adaption strategies by implementing effective mitigation measures to cope with the adverse effects of extreme droughts. For instance, the MoA has adopted modern water harvesting strategies and has increased the knowledge and expertise among farmers about the need to move toward the most drought-resistant farming systems (MoA 2016). Elsewhere, the PWA has initiated many interventional initiatives such as the Strategy for the Water and Wastewater Sector, the Draft Water Resources Management Strategy, the National Water Policy, Water Sector Strategy Planning Study (WSSPS), the Coastal Aquifer Management Program (CAMP), the National Water Plan (NWP), the Stormwater Infiltration Plan, Gaza Emergency Technical Assistance Program (GETAP) on Water Supply to the Gaza Strip, and the Comparative Study of Water Supply Options for the Gaza Strip (CSO-G) to maintain the integrity of the coastal aquifer and to alleviate the impacts of extreme drought events and water scarcity. These studies suggest the use of nonconventional water supplies such as recycled wastewater, desalinated seawater, and collected stormwater as an effective potential water resource in the water cycle to satisfy water demands and to mitigate drought consequences. Furthermore, in response to the drought episode of 2010–2011, the Water Scarcity Task Force (WSTF) was established as a new institutional framework to improve coordination between government agencies and to coordinate and manage data accessibility under extreme conditions to facilitate the practice of multiple humanitarian and emergency measures (WSTF 2011). The Gaza Strip

suffers from the lack of real data-based forecasting models that could be used for simulating future drought in the Gaza Strip. Specifically, Gampe *et al.* (2016) provided a predication for future drought in the Gaza Strip; however, the model's accuracy is contingent on getting image data from satellites and the correlation of the model does not exceed 55%. Therefore, the study's novelty is wrapped up in its ability to provide a reliable simulation model for the future based on the study of real acquired data from working meteorological stations in the Gaza Strip.

MATERIAL AND METHODS

The methodology of this study is to describe fluctuating drought patterns in the Gaza Strip using stochastic time-series modeling to integrate a comprehensive spatial and temporal spread of droughts over previous periods and the commencing 20 years. This approach is illustrated in Figure 5.

The target period of 20 years, up to the year 2040, is based on the expectation that current and proposed water resource management plans would be comprehensively in operation within the next 10–20 years. Therefore, simulating drought behavior over the target period is anticipated to guide policymakers to evaluate response efficiency for coastal aquifer sustainability and drought resilience measures.

Data collection and analysis

Daily rainfall data between 1974 and 2016 were collected, screened, and statistically analyzed through the nine
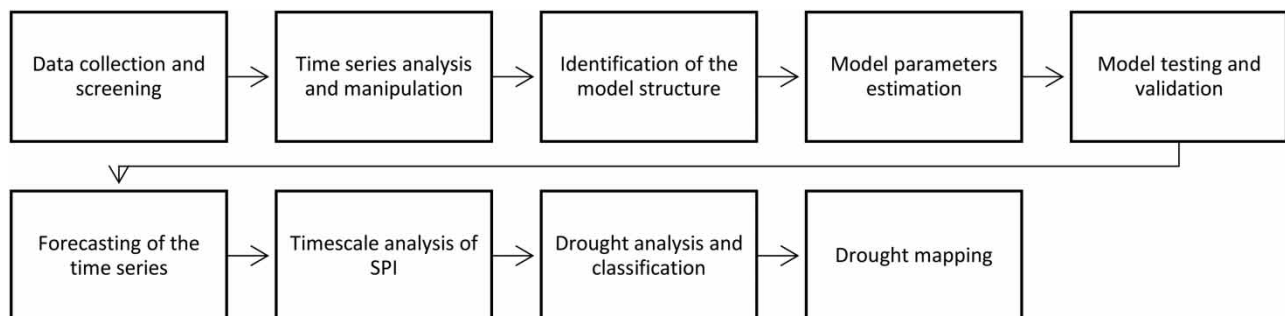

Figure 5 | Flowchart of the study's methodology.

meteorological stations of Beit Hanon, Beit Lahia, Shati, Remal, Mughraka, Nussirat, Deir Al-Balah, Khanyounis, and Rafah. The meteorological stations, as depicted in Figure 1, are well distributed across the entire geographical area to record the sensitivity of the distribution of rainfall from the south to the north of the Gaza Strip. The statistical analysis for the data, as shown in Table 2, shows that there is a prevalence of zero-rainfall in the summer, and the average monthly rainfall over the Gaza Strip is estimated at 21–39 mm. In the rainy season, the significant portion of rainfall drops, and it may reach a monthly average of around 135–330 mm. The findings indicate that in certain seasons, the Gaza Strip recorded massive quantities of rainwater. The statistical analysis demonstrates that the maximum rainfall values could reach a value of about 1.5–2.5 higher than the upper limit of outliers, which strongly confirms that during certain historical periods the Gaza Strip experienced floods. The average falling rainfall is distributed between 253 and 468 mm per annum, and the total annual volume of water that dropped in the Gaza Strip amounts to 92–171 million cubic meters.

Regionally, the northern Gaza Strip governorates contribute more to the recharge of the coastal aquifer than the southern governorates; therefore, all of the projects for infiltration and water harvesting and storage are planned for location in the northeastern regions of the Gaza Strip.

Analysis and manipulation of time series and model structuring

For the purposes of quality control and quality assurance, both R-statistical analysis language and the Statistical Package for Social Sciences (SPSS) were used in this research to evaluate the nature of the rainfall time series. The R-statistical analysis language is highly recommended for the purposes of climatic studies because of the vast availability of case studies. The SPSS is a familiar and established tool to confirm the consistency of results. The information inherent in the time-series data was derived through the analysis of the ACF, PACF, and the power spectrum. For the observed time series at the Beit Hanon station, the depicted ACF in Figure 6(a) shows a slow decay correlogram in a sinusoidal shape, which indicates that the data are in strong correlation with each other. The stationarity null hypostasis for the rainfall time series was tested using the Augmented Dickey–Fuller (ADF) test (Dickey & Fuller 1979). The *t*-statistic test gives a *p*-value of less than 5%; therefore, the null hypothesis is rejected, and this implies that the time series is stationary. The highlighted correlogram in Figure 6(a) illustrates that after a long time-lag of about 300 months, the correlation between the time series values becomes statistically insignificant at a significance level (α) of 95%, and this means that the time series should be converted into a more stationary form to extract the order of the MA components to structuring the

Table 2 │ Geographical location and statistical analysis for the meteorological stations of the Gaza Strip

| No. | Station name | Latitude °N | Longitude °E | Rainfall (mm per month) | | | | | |
				Minimum	25th percentile	50th percentile	75th percentile	Maximum	Standard deviation
1	Beit Hanon	31.5404	34.5404	0	0	39	57	330	58
2	Beit Lahia	31.5633	34.4695	0	0	36	53	325	52
3	Shati	31.5365	43.4459	0	0	33	54	237	47
4	Remal	31.5180	34.4425	0	0	33	48	255	46
5	Mughraka	31.4700	34.4254	0	0	31	47	287	46
6	Nussirat	31.4341	34.3891	0	0	30	49	253	42
7	Deir Al-Balah	31.4113	34.3438	0	0	28	46	172	38
8	Khanyounis	31.3412	34.3094	0	0	24	38	135	34
9	Rafah	31.2691	34.2563	0	0	21	35	155	30

time-series ARIMA model. The PACF expresses the degree of dependency of data on each other, and the PACF in Figure 6(b) reveals that 41% of the information in the time series is interpreted by the first observed value while the remaining 59% of the information is represented by the other observations.

The power spectrum, presented in Figure 6(c), implies that the time series explicitly repeats itself substantially every 12, 6 and 4 months. The statistical test at these spikes was significantly higher than the *F*-statistic test, and this reflects that the periodic pattern dominates the time series. To recapitulate, the original time series ought to be more stochastic in its behavioral process; therefore, the time series was processed and modified by inserting the series into a first-order seasonal differentiation to remove the substantial dependency of data on one another and the excessive periodicity. The modified time series for rainfall observations at the Beit Hanon meteorological station were reanalyzed through the ACF, PACF, and the spectrum as shown in Figure 4(a)′, (b)′, and (c)′, respectively. Generally, the identical analysis for all the rainfall observations at all meteorological stations implies that a seasonal ARIMA model (p, d, q) (P, D, Q)$_s$ of order (4,0,1) (5,1,1)$_{12}$ is the suitable structure to represent and to forecast the

rainfall time-series records at the Gaza Strip meteorological stations. In term of processing time, the model introduces the simulation results within a reasonable period of time. Moreover, a unique model was chosen to represent the simulation process at each station to mitigate the inaccuracies that could result from the redundancy of the structured models.

Model parameters estimation and validation

The algorithms of the R-statistical analysis language were utilized to investigate the structure of the stochastic models for each of the observed rainfall time series at each of the nine meteorological stations. The nonseasonal and seasonal components of AR and MA for the configured stochastic seasonal ARIMA (4,0,1) (5,1,1)$_{12}$ were specified for each of the nine rainfall time series as summarized in Table 3.

The seasonal ARIMA models were calibrated using 90% of the data, while the validation was performed on the remaining 10% of the data to test the performance of the models to forecast projections as shown in Figures 7 and 8. The degree of interpretation of simulated values to the observed values was investigated by the statistical measures of root mean squared error (RMSE) and *r*, which
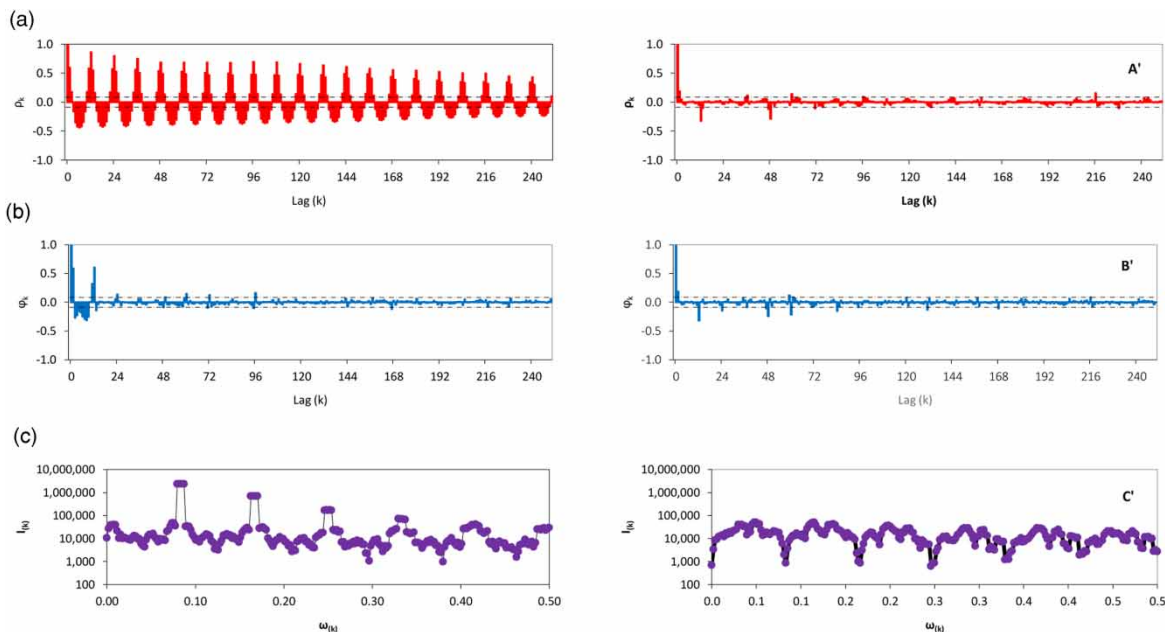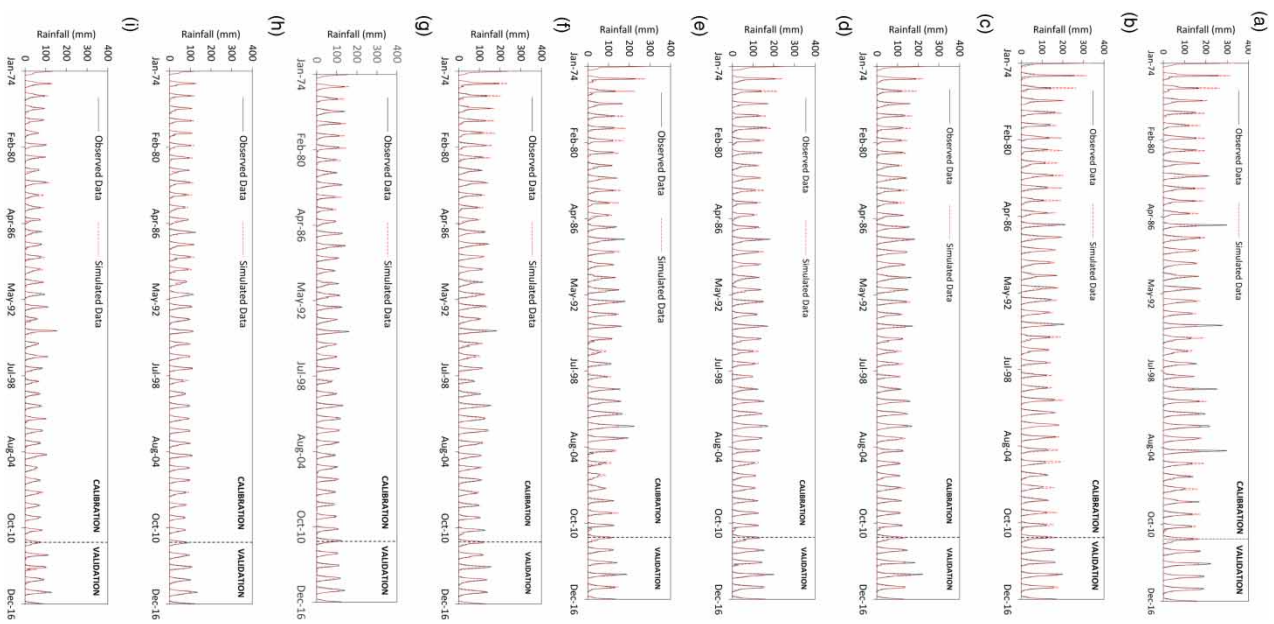

Figure 6 | Original and modified time-series analysis through (a and a′) correlogram; (b and b′) partial autocorrelation; and (c and c′) power spectrum.

Table 3 | The model AR and MA parameters at the meteorological stations of the Gaza Strip

No.	Station	Nonseasonal parameters					Seasonal parameters					
		Φ_1	Φ_2	Φ_3	Φ_4	θ_1	Φ_{1s}	Φ_{2s}	Φ_{3s}	Φ_{4s}	Φ_{5s}	θ_{1s}
1	Beit Hanon	0.0898	0.0681	−0.009	−0.0305	0.0815	0.2359	0.0021	−0.0139	−0.3537	−.0782	−0.8506
2	Beit Lahia	0.3608	0.0516	−0.0196	−0.0779	−0.0929	0.3267	0.0653	−0.0439	−0.2250	0.0796	−0.8178
3	Shati	0.2641	0.0808	0.0193	−0.0671	0.0735	0.1518	0.1523	−0.0801	−0.1707	−0.0045	−0.9837
4	Remal	0.1995	0.1352	0.0625	−0.0704	0.1095	0.0861	0.2789	−0.1438	−0.3245	0.0055	−0.8287
5	Mughraka	0.0457	0.1318	0.0257	−0.0432	0.1678	0.4013	0.1074	−0.1434	−0.2733	0.1393	−0.9036
6	Nussirat	0.0510	0.2433	−0.0378	−0.0890	0.4172	0.1299	0.0133	−0.0501	−0.2135	0.0325	−0.6948
7	Deir Al-Balah	−0.0159	0.2513	−0.0113	−0.1213	0.4451	−0.0094	−0.1093	−0.0860	−0.2455	0.0400	−0.7165
8	Khanyounis	−0.2557	0.4912	−0.1190	−0.1417	0.8434	0.1526	0.0167	0.0549	−0.1731	0.0189	−0.7284
9	Rafah	−0.1165	0.0574	0.0369	−0.0352	0.3698	0.1569	0.1573	0.1102	−0.3217	−0.0685	−0.9995

Figure 7 | The models performance at (a) Beit Hanon; (b) Beit Lahia; (c) Shati; (d) Remal; (e) Mughraka; (f) Nussirat; (g) Deir Al-Balah; (h) Khanyounis; and (i) Rafah.

demonstrates the power of correlation between the simulated and observed data. The data fitted in the model calibration range implies that the model correlation was around 93–97% of the response data variability around its mean. In particular, the model exhibits good behavior in the forecasting framework where model testing reveals that the model can predict future conditions with a
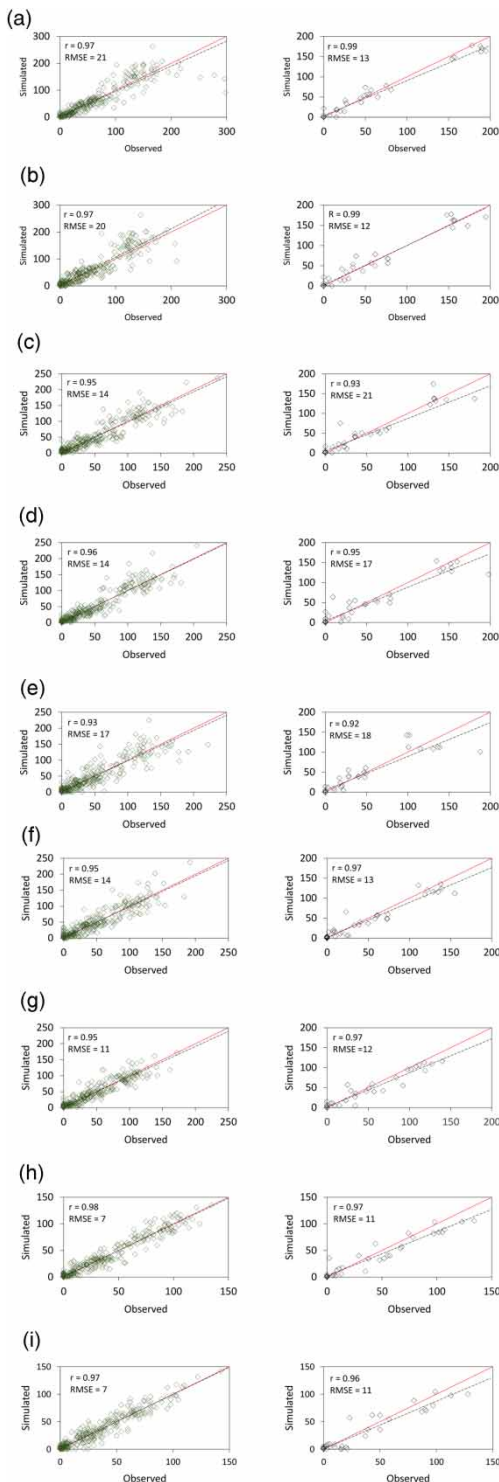
Figure 8 | The models performance at (a) Beit Hanon; (b) Beit Lahis; (c) Shati; (d) Remal; (e) Mughraka; (f) Nussirat; (g) Deir Al-Balah; (h) Khanyounis; and (i) Rafah.

predictive correlation accuracy of about 92–99%. In other cases, the correlation between the observed and the

simulated data is classified as a high correlation where in term of RMSE, the correlation strength in the calibration range is about 7–21, and a correlation of about 11–21 is provided in the validation test.

The Gaza Strip is a limited area of land so a unified structure of stochastic seasonal ARIMA model is deemed adequately appropriate for simulating the distribution of rainfall as well as simplifying data handling and reducing the inaccuracies that could emerge from using a myriad of models.

Drought analysis and classification

Devoting a clear framework for national-scale monitoring and evaluation of drought is a major challenge in articulating the impacts of climate change that directly threaten the coastal aquifer resilience and agricultural resources in the Gaza Strip. Intrinsically, the water budget appraisals in the Gaza Strip are prepared on an annual basis; therefore, it is more convenient to develop an annual national drought index to empower decision-makers to align the deficit and surplus in national water resources. Consequently, the SPI was evaluated on an annual basis every 12 months after compiling the historical data and simulating data over the following 20 years to 2040, using the previously mentioned stochastic seasonal ARIMA models. The annual SPI_{12} was computed at each of the nine meteorological stations to demonstrate the change in drought models due to the change in the rainfall patterns over the specified period. The rainfall threshold value that aligns the zero SPI_{12} and defines the separable limit between the state of dryness and wetness was specified by matching the rainfall and the SPI_{12} graphs of the CDF as shown in Figure 9. The rainfall threshold level rises regionally from 250 mm in the south to around 474 mm in the north of the Gaza Strip. Therefore, a mean rainfall threshold level of 370 mm was considered as a credible local reference scale in this study to assess the temporal and spatial dispersion of drought in the area of the Gaza Strip.

The comparative review for the matching graphs of the cumulative probability distribution for the rainfall and SPI at each of the meteorological stations indicates that the
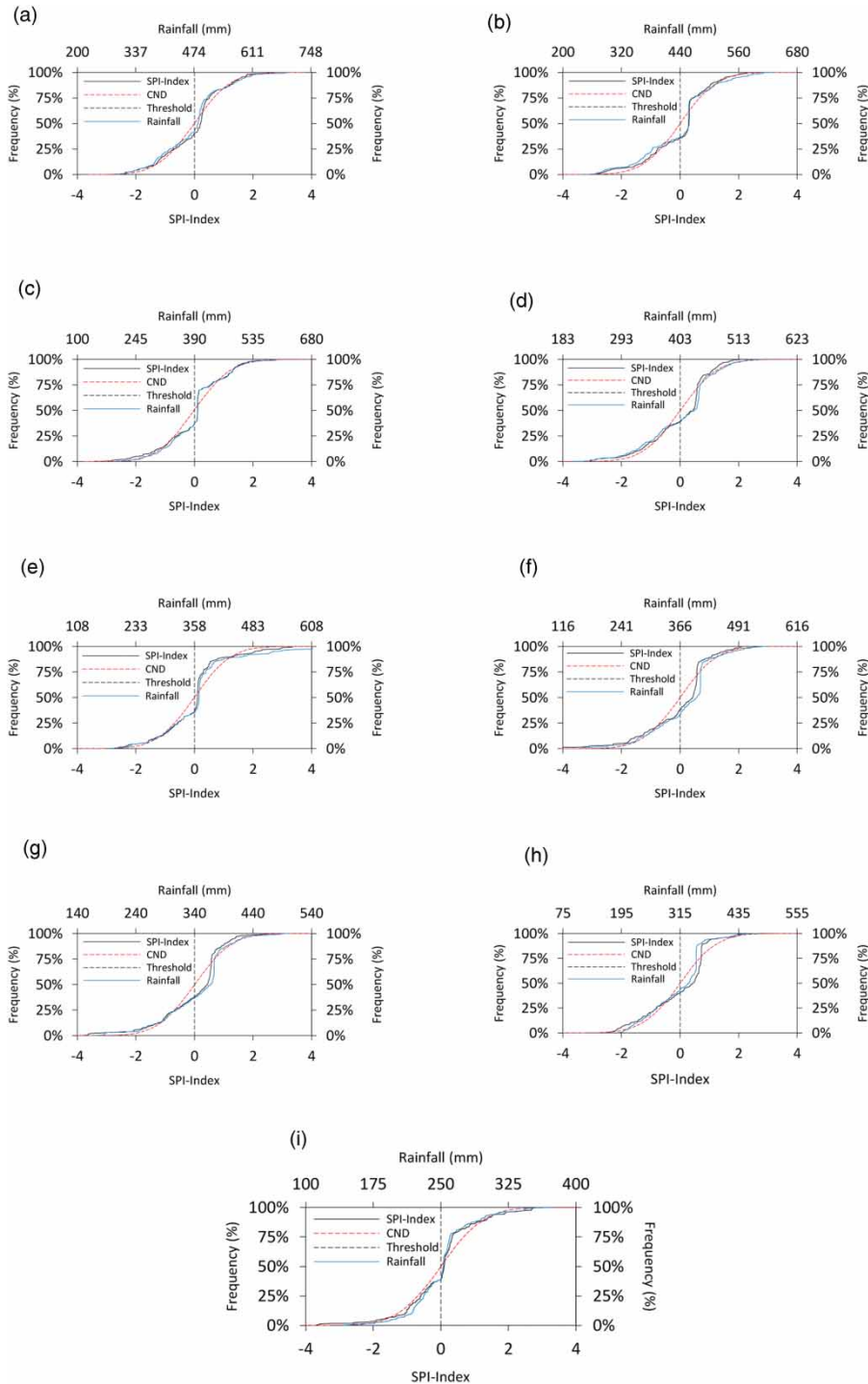
Figure 9 │ Matching the graphs of the normal distribution, CND functions and rainfall threshold levels for the meteorological stations of (a) Beit Hanon; (b) Beit Lahia; (c) Shati; (d) Remal; (e) Mughraka; (f) Nussirat; (g) Deir Al-Balah; (h) Khanyounis; and (i) Rafah.

representative local drought scale for the Gaza Strip could be established by fitting a probability rainfall distribution function with a mean and variance of 370 mm and 3,932, respectively, to match a probability SPI distribution function with a zero mean and a variance of 1, as shown in Figure 10.
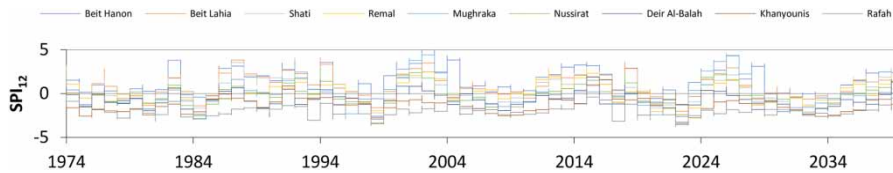
Figure 10 | 12-month scale for the meteorological stations of (a) Beit Hanon; (b) Beit Lahia; (c) Shati; (d) Remal; (e) Mughraka; (f) Nussirat; (g) Deir Al-Balah; (h) Khanyounis; and (i) Rafah.

According to the generated local drought SPI scale, the SPI_{12} for the rainfall time series at each of the nine meteorological stations was recomputed as the shown sample in Figure 10 for Beit Hanon and Rafah stations. The simulation of the rainfall over the coming 20 years shows stability in the SPI with some interruptions. Specifically, for the Gaza Strip, conditions are classified as extreme drought when annual rainfall is less than 230 mm. Meanwhile, for rainfall of 230–265, 265–300, and 300–370 mm, the drought is categorized as a severe, moderate, and normal drought, respectively. Likewise, the wet state may be defined by the amount of precipitation that exceeds the threshold value of 370 mm per year. The temporal distribution of the drought SPI_{12} over the years 1974–2040 reveals that the Gaza Strip witnessed drought conditions in the past and that the drought may also be described as chronic at some of the southern sites of the Gaza Strip.

RESULTS AND DISCUSSION

The consequences of climate change in MENA's Eastern Mediterranean countries are demonstrated dramatically by the rise in temperature compared with the decrease in precipitation. Analyzing the SPEI drought index shows that the drought status in the Eastern Mediterranean has shifted over the past 50 years from wet to severe drought. Moreover, the current probability of the incidence of drought is three times the probability than in the 1970s. At the regional level, the Gaza Strip area is facing severe drought with a probability of more than 80%. The lack of real field measurements due to weak possibilities and climate tracking programs is a major obstacle in the face of providing detailed prospects for the drought status in the Gaza Strip. In light of the scarcity of surveying studies about local drought conditions in the Gaza Strip, this study utilized the available data on precipitation to conduct a systematic

drought assessment over the past 46 years, in tandem with an assessment of the next 20 years. Employing the ability of the stochastic time-series models, the rainfall time series were presented using the stochastic seasonal ARIMA model of $(4,0,1)$ $(5,1,1)_{12}$ that shows a calibration accuracy of 93–97% and a future prediction accuracy of 92–99%. Based on the calibrated seasonal ARIMA models, the rainfall data were extended to the years of 2040. The trend analysis for the generated time series from historical and future rainfall implies that rainfall pattern is relatively consistent over the time frame in the northern governorates of Beit Hanon, Beit Lahia, Shati, and Remal. In contrast, the southern governorates of Mughraka, Nussirat, Deir Al-Balah, Khanyounis, and Rafah reveal a decreasing trend in the precipitation pattern, which confirms that the southern parts of the Gaza Strip are experiencing greater drought in the climatic conditions. More specifically, the annual SPI_{12} that was devised at each of the nine meteorological stations indicates that the rainfall threshold value decreases distinctly from the north to the south of the Gaza Strip. The annual precipitation threshold levels, which are the precipitation values of the no drought and no wet conditions, i.e., SPI = 0, were 474, 440, 390, 403, 358, 366, 340, 315, and 250 mm at the meteorological stations of Beit Hanon, Beit Lahia, Shati, Ramal, Mughraka, Nussirat, Deir Al-Balah, Khanyounis, and Rafah, respectively. In this study, to unify the comparison of the drought assessment investigations, a unified local SPI scale was established to provide a baseline comparative study to represent local drought conditions in the Gaza Strip. The local SPI scale was established at an annual precipitation threshold level of 370 mm, which demonstrates the droughtless condition at an SPI_{12} of zero. The temporal and spatial drought assessments that were mapped in Figure 11 confirm that the Gaza Strip faced serious evolving waves of drought over previous periods. The temporal assessment demonstrates that drought conditions distribute in an elliptic pattern over
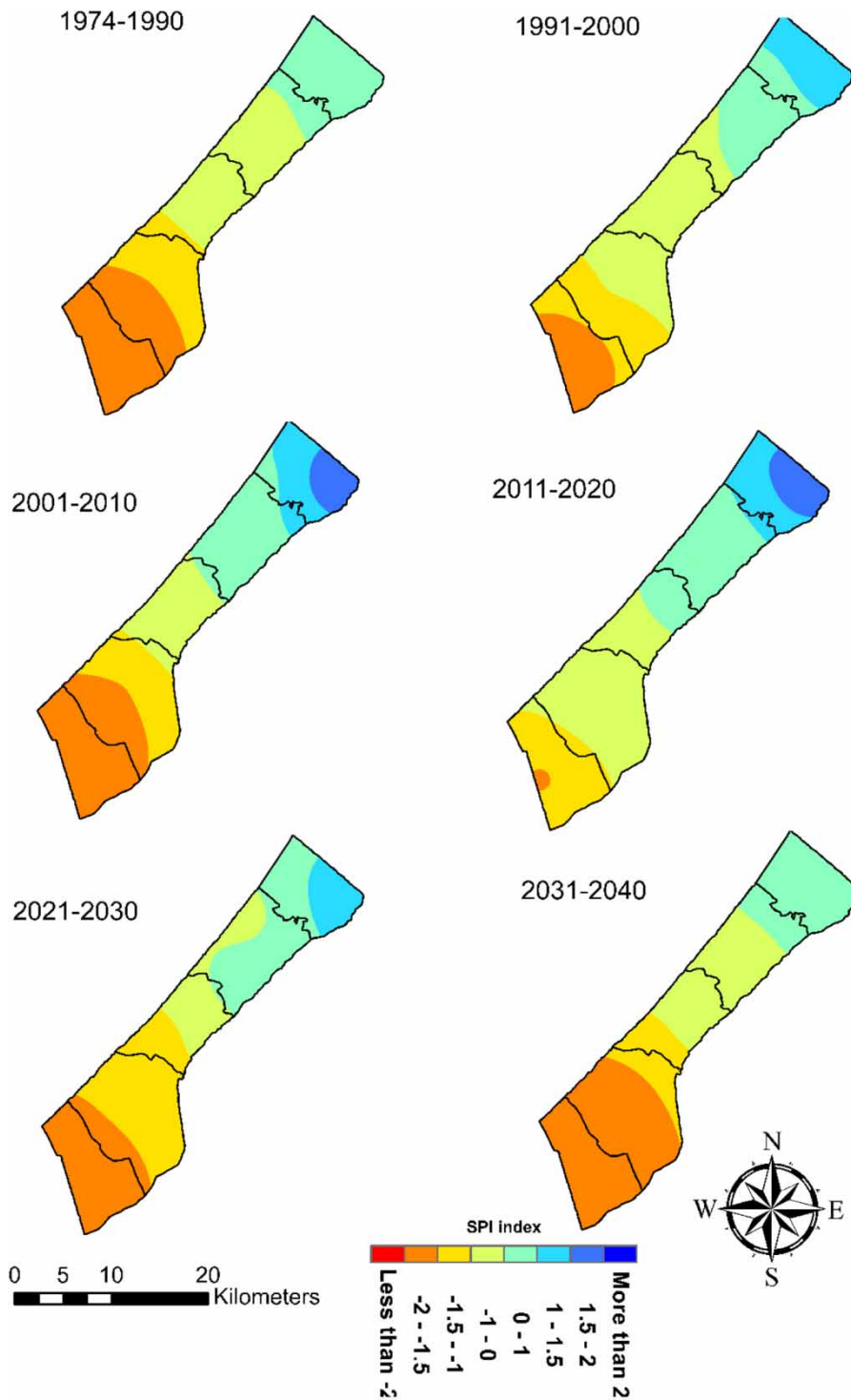
Figure 11 │ Drought propagation over the years from 1974 to 2040.

time, and the spatial distribution shows that the southern governorates of Khanyounis and Rafah are under extreme drought the majority of the time, as precipitation at these stations is less than average; the trend presenting in a decreasing pattern. The years of 1974, 1992, and 2016 were the most prosperous in terms of water. However, the

years of 1980, 1998, and 2010 were the most barren. On average, the next 20 years' drought conditions are to be severe in Rafah and Khanyounis with a rainfall amount of less than 230 mm per year. In central Gaza and Gaza, the dominant conditions are of moderate drought with an annual rainfall of 230–265 mm. The northern area of the Gaza Strip is forecasted to face moderate to normal drought with an annual rainfall of about 300–370 mm. The probabilistic analysis shown in Figure 12 signifies that the region of

the Gaza Strip risks drought status with a likely incidence rate that varies from 8% in the north to 100% in the south. The northern parts of the Gaza Strip have mostly precipitation levels above the specified average precipitation of 370 mm, and this is reflected in the low occurrence of drought. However, the precipitation of the southern parts of the Gaza Strip is almost below the average precipitation, and this leads to permanent drought in this area. More specifically, the normal drought is the prevalent drought in
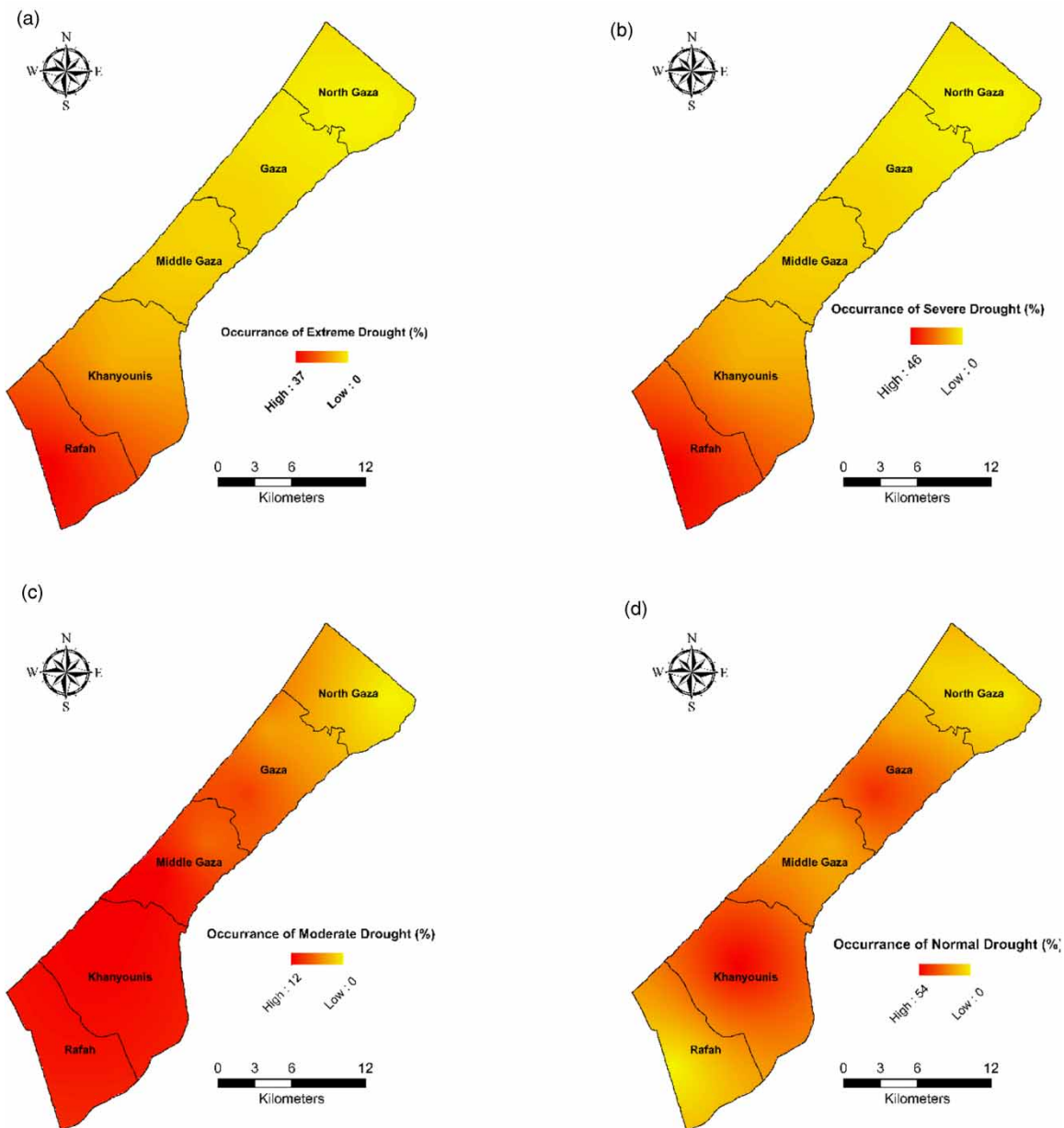

Figure 12 | Probability of drought occurrence for (a) extreme, (b) severe, (c) moderate, and (d) normal droughts.

the northern governorates, although the hazardous potential of extreme and severe drought is high in the southern governorates with an incidence risk of about 83%. Sequentially, southern governorates of Rafah and Khanyounis experience a chronic annual drought, while the period within which drought returns is reported to be every 9–12 years in the northern governorates of the Gaza Strip as depicted in Figure 13. The zoning of the Gaza Strip area reveals that 50% of the land experiences chronic drought events every year, while 28% of the Gaza Strip could face drought conditions every 2–3 years. Fifty percent of the land experiences chronic drought events every year, while 28% of the Gaza Strip could face drought conditions every 2–3 years. In this regard, the remaining 22% of the land endures drought with a return period of 3–12 years. In this context, the ongoing and future projections of drought reveal that urgent mitigation and intervention measures have to be taken to sustain the only available water resource of coastal aquifer in the Gaza Strip, which faces decline in the recharge process and is overexploited for domestic, agricultural, and other uses. In response, the PWA recommended water intervention strategies to maintain the quality of life in the Gaza Strip. The PWA suggests implementing a large-scale seawater desalination plant to be operated with the current short-term low volume seawater desalination plants in the Gaza Strip. The small-scale seawater desalination plants introduce about 7% of total water needs in the Gaza Strip. In addition, the large-scale central seawater desalination plant in Gaza is expected to provide 55 million cubic meters of the water in its first stage and about 110 million cubic meters in full operational capacity throughout the coming 20 years, which will improve the water situation by approximately 60% of total water needs. Moreover, the potential of reusing wastewater as a new water resource in the water cycle draws the attention of the PWA toward the willingness of implementing wastewater reclamation projects to exploit these resources in the replenishment of the coastal aquifer to remedy the impact of drought on groundwater sustainability. In the agricultural field, the PWA provided a plan to close all the illegal agricultural wells that exploit the aquifer arbitrarily and new irrigation systems were adopted to enable the farmers to use the reclaimed wastewater in the crops irrigating safely. Economically, the drought is expected to increase the price of water per unit;

therefore, prospective water supplies are going to be mainly dependent on the nonconventional water resources that need national investments in constructing the new assets. Environmentally, the drought in the Gaza Strip will have real impacts on the environment, and this emphasizes the need to establish an environmental monitoring program to monitor the quality of the environment. The construction of seawater desalination projects and operating wastewater reclamation projects is a direct reflection of the increase of greenhouse gas emissions in the environment, which increases global warming and hikes up global temperatures.

CONCLUSION AND RECOMMENDATION

Monitoring and forecasting the trend of climatic parameters reveal the impact of climate change on temporal and spatial distribution of droughts or flood events. The performance of the SPEI gives an accurate indication of drought interaction in terms of precipitation and temperature; however, the SPI reveals the conditions of drought depending on precipitation only. The robustness of stochastic models promotes these models as a simulator to mimic the pattern of observations and to forecast future conditions depending on the inherent trend of the time series. However, the stochastic models show significant deficiency in attaining outlier observations overcome by integrating other techniques like artificial neural networks. In this study, the stochastic models demonstrate high accuracy in modeling and forecasting the precipitation in the Gaza Strip due to low precipitation and low outlier measurements. The regional SPEI drought assessment for the Eastern Mediterranean region of MENA demonstrates that drought conditions in the Gaza Strip moved from the wet or nondrought conditions in the 1970s to moderate to severe drought within the last 10 years with an increase in drought occurrence probability of more than 40%. Locally, depending on the SPI scale and the adopted average precipitation amount by the PWA, the local temporal and spatial diagnostic assessment of drought is crucial to monitor the effectiveness of the anticipated national water supply projects that are planned to be implemented within the next 20 years to protect the sustainability of life in the Gaza Strip. Thus, the historical analysis demonstrates that the Gaza Strip faced serious
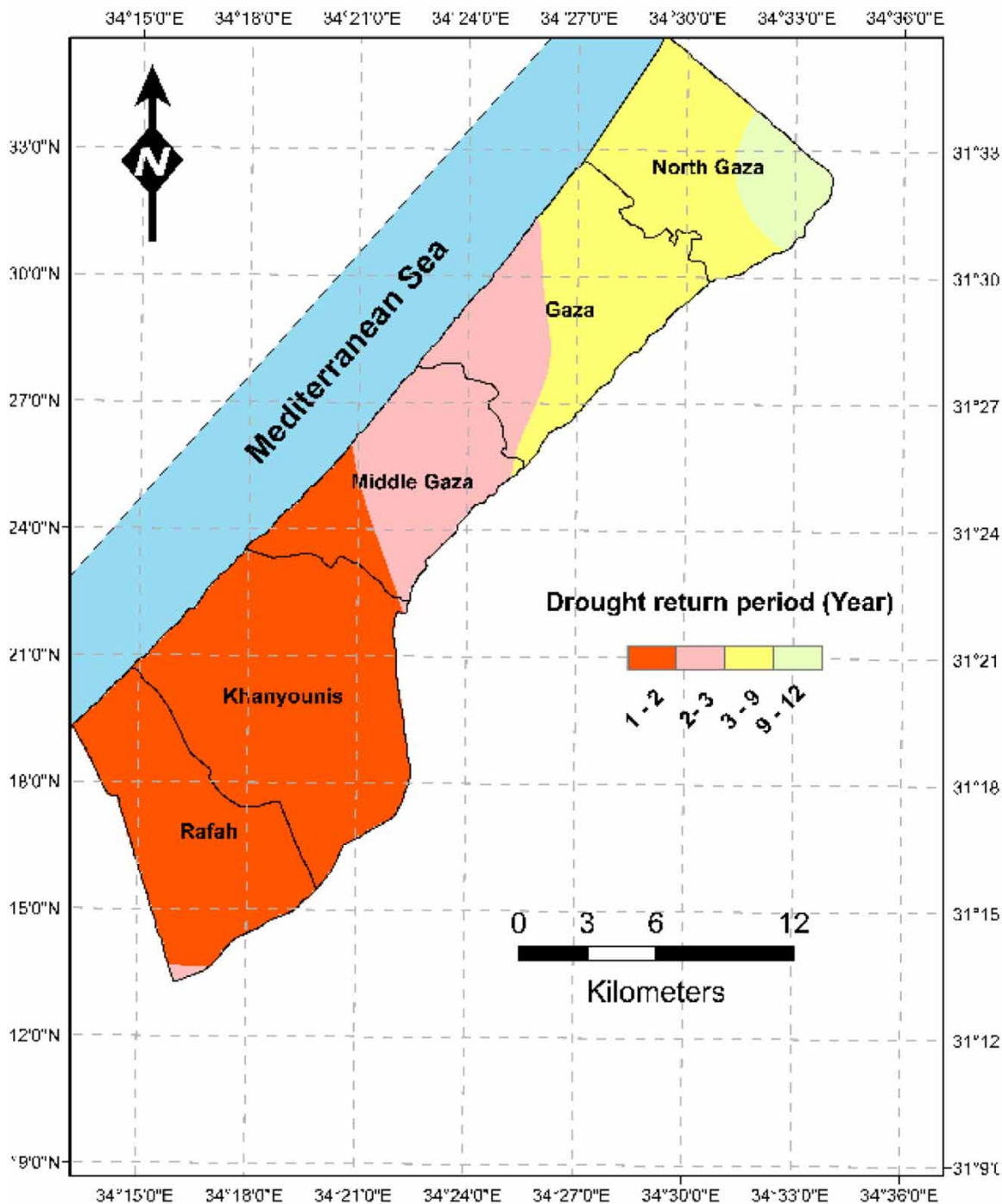
Figure 13 │ Drought return periods.

evolving drought conditions where, in general, the potential occurrence of drought conditions in the Gaza Strip ranges between 8% in the north, which faces considerable precipitation amounts almost higher than 370 mm per year, and 100% in the south, which bears chronic annual drought events due to the low precipitation conditions of

less than 370 mm per year. In conclusion, for the next 20 years, the drought pattern in the Gaza Strip is droughtless in the north with an average precipitation of about 433 mm per year, and normal to severe in the south with an average precipitation of about 242 mm per annum. The PWA adopted strategic water interventions to remedy the impact of hazardous drought over the forthcoming two decades. The principal part of these interventions is to operate a large-scale seawater desalination plant to decrease the deficit in water by about 60%. In addition, reclamation wastewater projects are to be completed to introduce water for groundwater recharge and agricultural irrigation.

DATA AVAILABILITY STATEMENT

All relevant data are included in the paper or its Supplementary Information.

REFERENCES

Abbaspour, K. C., Faramarzi, M., Ghasemi, S. S. & Yang, H. 2009 Assessing the impact of climate change on water resources in Iran. *Water Resources Research* **45** (10), 1–16. doi:10.1029/2008wr007615.

Abeysingha, N. S. & Rajapaksha, U. R. L. N. 2020 SPI-based spatiotemporal drought over Sri Lanka. *Advances in Meteorology* **2020**, 1–10. doi:10.1155/2020/9753279.

Abramowitz, M. & Stegun, I. A. 1970 *Handbook of Mathematical Functions with Formulas, Graphs, and Mathematical Tables*. Dover Publications, Inc., New York, NY, USA.

Abualtayef, M., Rahman, G. A., Snounu, I., Qahman, K., Sirhan, H. & Seif, A. K. 2017 Evaluation of the effect of water management interventions on water level of Gaza coastal aquifer. *Arabian Journal of Geosciences* **10** (24). doi:10.1007/s12517-017-3329-x.

AghaKouchak, A., Feldman, D., Stewardson, M. J., Saphores, J. D., Grant, S. & Sanders, B. 2014 Australia's drought: lessons for California. *Science* **343**, 1430–1431.

Aladaileh, H., Al Qinna, M., Barta, K., Al-Karablieh, E., Rakonczai, J. & Alobeiaat, A. 2019 A drought adaptation management system for groundwater resources based on combined drought index and vulnerability analysis. *Earth Systems and Environment* **3**, 445–461. doi:10.1007/s41748-019-00118-9.

Alamgir, M., Shahid, S., Mohsenipour, M. & Ahmed, K. 2015 Return periods of extreme meteorological droughts during

monsoon in Bangladesh. *Applied Mechanics and Materials* **735**, 186–189. doi:10.4028/www.scientific.net/amm.735.186.

Almedeij, J. 2014 Drought analysis for Kuwait using standardized precipitation index. *The Scientific World Journal* **2014**, 1–9. doi:10.1155/2014/451841.

Alqaysi, N. H. H., Dursun, S. & Almuslehi, M. A. A. 2017 Estimating drought index using standardized precipitation index from 1901 to 2015, Turkey. *Journal of International Environmental Application and Science* **12** (3), 154–160.

Al-Qinna, M. I., Hammouri, N. A., Obeidat, M. M. & Ahmad, F. Y. 2010 Drought analysis in Jordan under current and future climates. *Climatic Change* **106** (3), 421–440. doi:10.1007/s10584-010-9954-y.

Anshuka, A., van Ogtrop, F. F. & Willem Vervoort, R. 2019 Drought forecasting through statistical models using standardised precipitation index: a systematic review and meta-regression analysis. *Natural Hazards*. doi:10.1007/s11069-019-03665-6.

Avilés, A., Célleri, R., Solera, A. & Paredes, J. 2016 Probabilistic forecasting of drought events using Markov Chain- and Bayesian network-based models: a case study of an Andean Regulated River Basin. *Water* **8** (2), 37. doi:10.3390/w8020037.

Awchi, T. A. & Kalyana, M. M. 2017 Meteorological drought analysis in northern Iraq using SPI and GIS. *Sustainable Water Resources Management* **3** (4), 451–463. doi:10.1007/s40899-017-0111-x.

Banerjee, O., Bark, R., Connor, J. & Crossman, N. D. 2013 An ecosystem services approach to estimating economic losses associated with drought. *Ecological Economics* **91**, 19–27. doi:10.1016/j.ecolecon.2013.03.022.

Baruga, C. K., Kim, D. & Choi, M. 2020 A national-scale drought assessment in Uganda based on evapotranspiration deficits from the Bouchet hypothesis. *Journal of Hydrology* **580**, 1–44. doi:10.1016/j.jhydrol.2019.124348.

Bazrafshan, O. 2007 *Management and mapping drought hazard using standard precipitation Index (SPI) (case study: Golestan province)*. 2nd International Conference on Integrated Natural Disaster management, Tehran, Iran.

Bazrafshan, O., Salajegheh, A., Bazrafshan, J., Mahdavi, M. & Marj, A. F. 2015 Hydrological drought forecasting using ARIMA models (case study: Karkheh Basin). *ECOPERSIA* **3** (3), 1099–1117.

Behrangi, A., Nguyen, H. & Granger, S. 2015 Probabilistic seasonal prediction of meteorological drought using the bootstrap and multivariate information. *Journal of Applied Meteorology and Climatology* **54** (7), 1510–1522.

Box, G. E. P. & Jenkins, G. M. 1970 *Time Series Analysis, Forecasting and Control, rev. ed.* Holden-Day, San Francisco.

Box, G. E. P. & Jenkins, G.M. 1976 *Time Series Analysis: Forecasting and control, rev. ed.* Holden-Day, San Francisco.

Box, G. E. P., Jenkins, G. M. & Reinsel, G. C. 2008 *Time Series Analysis: Forecasting and Control*, 4th edn. Wiley Series in Probability and Statistics, Wiley, Hoboken, NJ.

Byun, H. R. & Wilhite, D. A. 1999 Objective quantification of drought severity and duration. *Journal of Climate* **12** (9),

2747–2756. doi:10.1175/1520-0442(1999)012 < 2747: oqodsa > 2.0.co;2.

Caloiero, T., Veltri, S., Caloiero, P. & Frustaci, F. 2018 Drought analysis in Europe and in the Mediterranean basin using the standardized precipitation index. *Water* **10** (8), 1043. doi:10.3390/w10081043.

Cancelliere, A. & Salas, J. D. 2004 Drought length properties for periodic-stochastic hydrologic data. *Water Resources Research* **40** (2), 1–13. doi:10.1029/2002wr001750.

Cancelliere, A., Mauro, G. D., Bonaccorso, B. & Rossi, G. 2007 Stochastic forecasting of drought indices. In: *Methods and Tools for Drought Analysis and Management. Water Science and Technology Library*, Vol. 62 (G. Rossi, T. Vega & B. Bonaccorso, eds). Springer, Dordrecht. doi:10.1007/978-1-4020-5924-7_5.

Chatfield, C. 2003 *The Analysis of Time Series: An Introduction*, 6th edn. A CRC Press Company of Taylor and Francis Group, New York.

Commonwealth Scientific and Industrial Research Organisation (CSIRO Australia). Climate and water availability in south-eastern Australia: a synthesis of findings from Phase 2 of South Eastern Australian Climate Initiative (SEACI), CSIRO, Australia, September 2012, 41 pp. Available from: http://www. droughtmanagement.info/literature/ SEACI_Climate_Water_South_Eastern_Australia_2012.pdf (accessed 23 September 2014).

Cook, B. I., Anchukaitis, K. J., Touchan, R., Meko, D. M. & Cook, E. R. 2016 Spatiotemporal drought variability in the Mediterranean over the last 900 years. *Journal of Geophysical Research: Atmospheres* **121** (5), 2060–2074, doi:10.1002/2015JD023929.

Dai, A., Trenberth, K. E. & Qian, T. 2004 A global dataset of palmer drought severity index for 1870–2002: relationship with soil moisture and effects of surface warming. *American Meteorological Society, Journal of Hydrometeorology* **5** (6), 1117–1130. doi:10.1175/JHM-386.1.

Dell, M., Jones, B. F. & Olken, B. A. 2012 Temperature shocks and economic growth: evidence from the last half century: dataset. *American Economic Journal of Macroeconomics* **4** (3), 66–95.

Dentoni, M., Deidda, R., Paniconi, C., Qahman, K. & Lecca, G. 2014 A simulation/optimization study to assess seawater intrusion management strategies for the Gaza Strip coastal aquifer (Palestine). *Hydrogeology Journal* **23** (2), 249–264. doi:10.1007/s10040-014-1214-1.

Dickey, D. A. & Fuller, W. A. 1979 Distribution of the estimators for autoregressive time series with a unit root. *Journal of the American Statistical Association* **74** (366a), 427–431. doi:10.1080/01621459.1979.10482531.

Djerbouai, S. & Souag-Gamane, D. 2016 Drought forecasting using neural networks, wavelet neural networks, and stochastic models: case of the Algerois Basin in North Algeria. *Water Resources Management* **30** (7), 2445–2464. doi:10.1007/s11269-016-1298-6.

Doroszkiewicz, J., Romanowicz, R. J. & Kiczko, A. 2019 The influence of flow projection errors on flood hazard estimates in future climate conditions. *Water* **11** (1), 49–68. doi.org/10.3390/w11010049.

Du, L., Tian, Q., Yu, T., Meng, Q., Jancso, T., Udvardy, P. & Huang, Y. 2013 A comprehensive drought monitoring method integrating MODIS and TRMM data. *International Journal of Applied Earth Observation and Geoinformation* **23**, 245–253. doi:10.1016/j.jag.2012.09.010.

Efstathiou, M. N. & Varotsos, C. A. 2012 Intrinsic properties of Sahel precipitation anomalies and rainfall. *Theoretical and Applied Climatology* **109** (3–4), 627–633. doi: 10.1007/s00704-012-0605-2.

Elasha, B. O. 2010 Mapping of climate change threats and human development impacts in the Arab Regions. In *Arab Human Development Report Research Paper Series*. UNDP, New York.

El Baba, M., Kayastha, P., Huysmans, M. & De Smedt, F. 2020 Evaluation of the groundwater quality using the water quality index and geostatistical analysis in the Dier al-Balah Governorate, Gaza Strip, Palestine. *Water* **12** (1), 262. doi:10.3390/w12010262.

El Kenawy, A., McCabe, M., Vicente-Serrano, S., Robaa, S. & Lopez-Moreno, J. 2016 Recent changes in continentality and aridity conditions over the Middle East and North Africa region, and their association with circulation patterns. *Climate Research* **69** (1), 25–43. doi:10.3354/cr01389.

Elkollaly, M., Khadr, M. & Zeidan, B. 2017 Drought analysis in the Eastern Nile basin using the standardized precipitation index. *Environmental Science and Pollution Research*. doi:10.1007/s11356-016-8347-9.

FAO 2018 *Drought Characteristics and Management in North Africa and the Near East*. FAO Water Reports, Food and Agricultural Organization of the United Nations, Rome.

FEMA 1995 *National Mitigation Strategy*. Federal Emergency Management Agency, Washington, DC.

Fung, K. F., Huang, Y. F., Koo, C. H. & Mirzaei, M. 2019 Improved SVR machine learning models for agricultural drought prediction at downstream of Langat River Basin, Malaysia. *Journal of Water and Climate Change*. doi:10.2166/wcc.2019.295.

Gampe, D., Ludwig, R., Qahman, K. & Afifi, S. 2016 Applying the triangle method for the parameterization of irrigated areas as input for spatially distributed hydrological modeling – assessing future drought risk in the Gaza Strip (Palestine). *Science of The Total Environment* **543**, 877–888. doi:10.1016/j.scitotenv.2015.07.098.

Gaur, A., Gaur, A. & Simonovic, S. 2018 Future changes in flood hazards across Canada under a changing climate. *Water* **10** (10), 1441–1462. doi:10.3390/w10101441.

Gibbs, W. J. & Maher, J. V. 1967 *Rainfall Deciles as Drought Indicators*. Melbourne: Bureau of Meteorology 44. pp. 84 Bulletin No. 48. Australia.

Golmohammadian, H. & Pishvaei, M. R. 2014 Evaluation displacement of upper envelope subtropical high over Iran in the 1948–2010 period. In: *Paper presented at the 16th Iran*

Geophysics Conference. Iranian Geophysical Conference, Tehran.

Gupta, A. K., Nair, S. S., Ghosh, O., Singh, A. & Dey, S. 2014 Bundelkhand Drought: Retrospective Analysis and Way Ahead. National Institute of Disaster Management, New Delhi, p. 148.

Guttman, N. B. 1998 Comparing the palmer drought index and the standardized precipitation index. Journal of the American Water Resources Association 34 (1), 113–121. doi:10.1111/j. 1752-1688.1998.tb05964.x.

Habibi, B., Meddi, M., Torfs, P. J. J. F., Remaoun, M. & Van Lanen, H. A. J. 2018 Characterisation and prediction of meteorological drought using stochastic models in the semi-arid Chéliff–Zahrez basin (Algeria). Journal of Hydrology: Regional Studies 16, 15–31. doi:10.1016/j.ejrh.2018.02.005.

Halwatura, D., McIntyre, N., Lechner, A. M. & Arnold, S. 2017 Capability of meteorological drought indices for detecting soil moisture droughts. Journal of Hydrology: Regional Studies 12, 396–412. doi:10.1016/j.ejrh.2017.06.001.

Hameed, M., Ahmadalipour, A. & Moradkhani, H. 2020 Drought and food security in the Middle East: an analytical framework. Agricultural and Forest Meteorology 281, 107816. doi:10.1016/j.agrformet.2019.107816.

Han, P., Wang, P. X., Zhang, S. Y. & Zhu, D. H. 2010 Drought forecasting based on the remote sensing data using ARIMA models. Mathematical and Computer Modelling 51 (11–12), 1398–1403. doi:10.1016/j.mcm.2009.10.031.

Han, J. & Singh, V. P. 2020 Forecasting of droughts and tree mortality under global warming: a review of causative mechanisms and modeling methods. Journal of Water and Climate Change 11 (3), 600–632. doi:10.2166/wcc.2020.239.

Hao, Z. & AghaKouchak, A. 2013 Multivariate standardized drought index: a parametric multi-index model. Advances in Water Resources 57, 12–18. doi:10.1016/j.advwatres.2013.03. 009.

Hao, Z., Hao, F., Singh, V. P., Sun, A. Y. & Xia, Y. 2016 Probabilistic prediction of hydrologic drought using a conditional probability approach based on the meta-Gaussian model. Journal of Hydrology 542, 772–780. doi:10. 1016/j.jhydrol.2016.09.048.

Hao, Z., Singh, V. P. & Xia, Y. 2018 Seasonal drought prediction: Advances, challenges, and future prospects. Reviews of Geophysics 56 (1), 108–141. doi:10.1002/2016rg000549.

Haque, M. M., Ahmed, A., Rahman, A. & Eslamian, S. 2017 Drought losses to local economy. In: Handbook of Drought and Water Scarcity: Principles of Drought and Water Scarcity (S. Eslamian & F. Eslamian, eds). pp. 627–641. Available from: https://ebookcentral.proquest.com/lib/uwsau/reader. action?docID=4935540&ppg=644.

Hauser, M., Gudmundsson, L., Orth, R., Jézéquel, A., Haustein, K., Vautard, R., Geert Jan van Oldenborgh, G. J. V., Wilcox, L. & Seneviratne, S. I. 2017 Methods and model dependency of extreme event attribution: the 2015 European drought. Earth's Future 5 (10), 1034–1043. doi:10.1002/ 2017ef000612.

Hingray, B., Picouet, C. & Musy, A. 2014 Hydrology A Science for Engineers. CRC Press, Taylor and Francis Group, New York.

Homdee, T., Pongput, K. & Kanae, S. 2016 A comparative performance analysis of three standardized climatic drought indices in the Chi River basin, Thailand. Agriculture and Natural Resources 50 (3), 211–219. doi:10.1016/j.anres.2016. 02.002.

Huang, Y., Gerber, S., Huang, T. & Lichstein, J. W. 2016 Evaluating the drought response of CMIP5 models using global gross primary productivity, leaf area, precipitation, and soil moisture data. Global Biogeochemical Cycles 30 (12), 1827–1846. doi:10.1002/2016gb005480.

Huttner, P. 2014 Climate cast: Is climate change estabilizing Iraq? In Updraft. Accessible at: https://blogs.mprnews.org/ updraft/2014/09/climate-cast-is-climatechange- destabilizing-iraq/ (Accessed 2nd April 2019).

IPCC 2007 Climate change 2007: synthesis report. In: Contribution of Working Groups I, II and III to the Fourth Assessment Report of the Intergovernmental Panel on Climate Change (Core Writing Team, R. K. Pachauri & A. Reisinger, eds). IPCC, Geneva, Switzerland, p. 104.

IPCC 2014 Climate change 2014: synthesis report. In: Contribution of Working Groups I, II and III to the Fifth Assessment Report of the Intergovernmental Panel on Climate Change (Core Writing Team, R. K. Pachauri & L. A. Meyer, eds). IPCC, Geneva, Switzerland, p. 151.

Issar, A. S. 2003 Climate Changes During the Holocene and Their Impact on Hydrological Systems. Cambridge University Press, New York.

Javanmard, S., Emamhadi, M., BodaghJamali, J. & Didehvarasl, A. 2017 Spatial –temporal analysis of drought in Iran using SPI during a long-term period. Earth Sciences. 6 (2), 15–29. doi:10.11648/j.earth.20170602.12.

Jouybari-Moghaddam, Y., Saradjian, M. R. & Forati, A. M. 2017 A probability model for drought prediction using fusion of Markov chain and Sax methods. In The International Archives of the Photogrammetry, Remote Sensing and Spatial Information Sciences, Vol. XLII-4/W4, pp. 101–104. https:// doi.org/10.5194/isprs-archives-XLII-4-W4-101-2017.

Kam, J., Kim, S. & Shao, W. 2019 Spatiotemporal patterns of US drought awareness. Palgrave Commun. 5, 107. https://doi. org/10.1057/s41599-019-0317-7.

Kampragou, E., Apostolaki, S., Manoli, E., Froebrich, J. & Assimacopoulos, D. 2011 Towards the harmonization of water-related policies for managing drought risks across the EU. Environmental Science and Policy 14 (7), 815–824. doi:10.1016/j.envsci.2011.04.001.

Karami, N. 2016 Factors of climate extremes hyperactivity: A study on MENA. International Journal of Geography and Regional Planning 2 (1), 011–026.

Karavitis, C. A., Vasilakou, C. G., Tsesmelis, D. E., Oikonomou, P. D., Skondras, N. A., Stamatakos, D., Fassouli, V. & Alexandris, S. 2015 Short-term drought forecasting combining stochastic and geo-statistical approaches. European Water 49, 43–63.

Kashyap, R. L. & Rao, A. R. 1976 Dynamic stochastic models from empirical data. In: *Mathematics in Science and Engineering* Vol. 122 (A. Kashyap, ed). Academic Press, Inc., London, UK, p. 334.

Keka, I. A., Matin, I., Rahman, M. & Banu, D. A. 2012 Analysis of drought in eastern part of Bangladesh. *Daffodil International University Journal of Science and Technology* 7 (1), 20–26. doi: 10.3329/diujst.v7i1.9643.

Kelley, C. P., Mohtadi, S., Cane, M. A., Seager, R. & Kushnir, Y. 2015 Climate change in the Fertile Crescent and implications of the recent Syrian drought. *Proceedings of the National Academy of Sciences* 112 (11), 3241–3246. doi:10.1073/pnas. 1421533112.

Keramat, A., Marivani, B. & Samsami, M. 2011 Climatic change, drought and dust crisis in Iran. *International Journal of Geological and Environmental Engineering* 5 (9), 472–475. doi.org/10.5281/zenodo.1058935.

Khan, N., Sachindra, D. A., Shahid, S., Ahmed, K., Shiru, M. S. & Nawaz, N. 2020 Prediction of droughts over Pakistan using machine learning algorithms. *Advances in Water Resources* 139, 103562. doi:10.1016/j.advwatres.2020.103562.

Khorasani, M., Ehteshami, M., Ghadimi, H. & Salari, M. 2016 Simulation and analysis of temporal changes of groundwater depth using time series modeling. *Modeling Earth Systems and Environment* 2 (2), 1–10. doi:10.1007/s40808-016-0164-0.

Kim, W., Iizumi, T. & Nishimori, M. 2019 Global patterns of crop production losses associated with droughts from 1983 to 2009. *Journal of Applied Meteorology and Climatology* 58 (6), 1233–1244. doi:10.1175/jamc-d-18-0174.1.

Kogan, F. N. 1995 Application of vegetation index and brightness temperature for drought detection. *Advances in Space Research* 15 (11), 91–100. doi:10.1016/0273-1177(95)00079-t.

Koopmans, L. H. 1974 *The Spectral Analysis of Time Series*. Academic Press, Inc., New York.

Kottegoda, N. T. 1980 *Stochastic Water Resources Technology*, 1st edn. Palgrave Macmillan, London, UK, p. 384

Kumbuyo, C. P., Yasuda, H., Kitamura, Y. & Shimizu, K. 2014 Fluctuation of rainfall time series in Malawi: an analysis of selected areas. *GEOFIZIKA* 31, 15–12. doi: 10.15233/gfz. 2014.31.

Kuswanto, H. & Naufal, A. 2019 Evaluation of performance of drought prediction in Indonesia based on TRMM and MERRA-2 using machine learning methods. *MethodsX* 6, 1238–1251. doi:10.1016/j.mex.2019.05.029.

Kwak, J., Kim, S., Jung, J., Singh, V. P., Lee, D. R. & Kim, H. S. 2016 Assessment of meteorological drought in Korea under climate change. *Advances in Meteorology* 1–13. doi:10.1155/ 2016/1879024.

Leblanc, M., Tweed, S., Van Dijk, A. & Timbal, B. 2012 A review of historic and future hydrological changes in the Murray-Darling Basin. *Global and Planetary Change* 80–81, 226–246. doi:10.1016/j.gloplacha.2011.10.012.

Lelieveld, J., Proestos, Y., Hadjinicolaou, P., Tanarhte, M., Tyrlis, E. & Zittis, G. 2016 Strongly increasing heat extremes in the Middle East and North Africa (MENA) in the 21st century.

Climatic Change 137, 245–260. https://doi.org/10.1007/ s10584-016-1665-6.

Low, K. G., Grant, S. B., Hamilton, A. J., Gan, K., Saphores, J.-D., Arora, M. & Feldman, D. L. 2015 Fighting drought with innovation: Melbourne's response to the Millennium Drought in Southeast Australia. *Wiley Interdisciplinary Reviews: Water* 2 (4), 315–328. doi:10.1002/wat2.1087.

Machiwal, D. & Jha, M. K. 2012 *Hydrologic Time Series Analysis: Theory and Practice*. Capital Publishing Company, India.

Madadgar, S., AghaKouchak, A., Shukla, S., Wood, A. W., Cheng, L., Hsu, K.-L. & Svoboda, M. 2016 A hybrid statistical-dynamical framework for meteorological drought prediction: application to the southwestern United States. *Water Resources Research* 52 (7), 5095–5110. doi:10.1002/2015wr018547.

Malik, A., Kumar, A., Salih, S. Q., Kim, S., Kim, N. W., Yaseen, Z. M. & Singh, V. P. 2020 Drought index prediction using advanced fuzzy logic model: regional case study over Kumaon in India. *PLoS ONE* 15 (5), e0233280. https://doi. org/10.1371/ journal.pone.0233280.

Manatsa, D., Mukwada, G., Siziba, E. & Chinyanganya, T. 2010 Analysis of multidimensional aspects of agricultural droughts in Zimbabwe using the Standardized Precipitation Index (SPI). *Theoretical and Applied Climatology* 102 (3–4), 287–305. doi:10.1007/s00704-010-0262-2.

Markus, M., Cai, X. & Sriver, R. 2019 Extreme floods and droughts under future climate scenarios. *Water* 11 (8), 1720–1725. doi:10.3390/w11081720.

McKee, T. B., Doesken, N. J. & Kleist, J. 1985 Drought monitoring with multiple time scales. In: *Proceedings of the 9th Conference on Applied Climatology*. American Meteorological Society, Dallas, TX, USA, pp. 233–236.

McKee, T. B., Doesken, N. J. & Kleist, J. 1993 The relationship of drought frequency and duration to time scales. In: *Proceedings of the Eighth Conference on Applied Climatology*. American Meteorological Society, Boston, MA.

McKee, T. B., Doesken, N. J. & Kleist, J. 1995 Drought monitoring with multiple time scales. In *Proceedings of the Ninth Conference on Applied Climatology*. American Meteorological Society, Boston, MA.

Mehr, A. D., Sorman, A. U., Kahya, E. & Afshar, M. H. 2019 Climate change impacts on meteorological drought using SPI and SPEI: case study of Ankara, Turkey. *Hydrological Sciences Journal* 65 (2), 254–268. doi:10.1080/02626667. 2019.1691218.

Mirzavand, M. & Ghazavi, R. 2015 A stochastic modelling technique for groundwater level forecasting in an arid environment using time series methods. *Water Resources Management* 29 (4), 1315–1328. doi:10.1007/s11269-014-0875-9.

Mishra, A. K. & Desai, V. R. 2005 Drought forecasting using stochastic models. *Stochastic Environmental Research and Risk Assessment* 19 (5), 326–339. doi:10.1007/s00477-005-0238-4.

Mishra, A. K. & Singh, V. P. 2010 A review of drought concepts. *Journal of Hydrology* 391 (1–2), 202–216. doi:10.1016/ j.jhydrol.2010.07.012.

MoA 2008 *Agricultural Water Scarcity Position Paper of the MoA*. Issued at 22 July, 2008, Palestine.

MoA 2016 *National Agricultural Sector Strategy (2017–2022): Resilience and Sustainable Development*. Ministry of Agriculture, Palestine.

Modarres, R. 2007 Streamflow drought time series forecasting. *Stochastic Environmental Research and Risk Assessment* **21** (3), 223–233. doi:10.1007/s00477-006-0058-1.

Modarres, R., Sarhadi, A. & Burn, D. H. 2016 Changes of extreme drought and flood events in Iran. *Global and Planetary Change* **144**, 67–81. doi:10.1016/j.gloplacha.2016.07.008.

Moghimi, M. M., Zarei, A. R. & Mahmoudi, M. R. 2019 Seasonal drought forecasting in arid regions, using different time series models and RDI index. *Journal of Water and Climate Change*. doi:10.2166/wcc.2019.009.

Mondol, M. H., Ara, I. & Das, S. D. 2017 Meteorological drought index mapping in Bangladesh using standardized precipitation index during 1981–2010. *Advances in Meteorology* **2017**, 1–17. https://doi.org/10.1155/2017/4642060.

Moreira, E. E., Martins, D. S. & Pereira, L. S. 2015 Assessing drought cycles in SPI time series using a Fourier analysis. *Natural Hazards and Earth System Sciences* **15** (3), 571–585. doi:10.5194/nhess-15-571-2015.

Morid, S., Smakhtin, V. & Moghaddasi, M. 2006 Comparison of seven meteorological indices for drought monitoring in Iran. *International Journal of Climatology* **26** (7), 971–985. doi:10.1002/joc.1264.

Mortensen, E., Wu, S., Notaro, M., Vavrus, S., Montgomery, R., De Piérola, J. & Block, P. 2018 Regression-based season-ahead drought prediction for southern Peru conditioned on large-scale climate variables. *Hydrology and Earth System Sciences* **22** (1), 287–303. doi:10.5194/hess-22-287-2018.

Munger, T. T. 1916 Graphic method of representing and comparing drought intensities. *Monthly Weather Review* **44** (11), 642–643.

Mushtaha, A. & Walraevens, K. 2018 Quantification of submarine groundwater discharge in the Gaza Strip. *Water* **10** (12), 1818. doi:10.3390/w10121818.

Myronidis, D., Ioannou, K., Fotakis, D. & Dörflinger, G. 2018 Streamflow and hydrological drought trend analysis and forecasting in Cyprus. *Water Resources Management* **32** (5), 1759–1776. doi:10.1007/s11269-018-1902-z.

Nagarajan, R. 2010 *Drought Assessment*. Springer, Netherlands, p. 429. doi:10.1007/978-90-481-2500-5.

Nam, W. H., Hayes, M. J., Svoboda, M. D., Tadesse, T. & Wilhite, D. A. 2015 Drought hazard assessment in the context of climate change for South Korea. *Agricultural Water Management* **160**, 106–117. https://doi.org/10.1016/j.agwat.2015.06.029.

Palmer, W. C. 1965 *Meteorological Drought*. U.S. Department of Commerce, Weather Bureau, Washington, DC, USA.

Palmer, W. C. 1968 Keeping track of crop moisture conditions, nationwide: the new crop moisture index. *Weather Wise* **21** (4), 156–161.

Paredes, F. J. & Guevara, E. 2013 A probabilistic model for the prediction of meteorological droughts in Venezuela. *Atmósfera* **26** (3), 311–323.

Patterson, L. A., Lutz, B. D. & Doyle, M. W. 2013 Characterization of drought in the South Atlantic, United States. *Journal of the American Water Resources Association* **49** (6), 1385–1397. https://doi.org/10.1111/jawr.12090.

PCBS 2020 *Estimated Population in the Palestinian Territory mid-Year by Governorate, 1997–2021*. IOP Publishing Physics Web. Available from: http://www.pcbs.gov.ps/Portals/_Rainbow/Documents/%D8%A7%D9%84%D9%85%D8%AD%D8%A7%D9%81%D8%B8%D8%A7%D8%AA%20%D8%A7%D9%86%D8%AC%D9%84%D9%8A%D8%B2%D9%8A%2097-2017.html (accessed 25 April 2020).

Petrasovits, I. 1990 General Review on Drought strategies. In: Transactions of 14th Congress on Irrigation and Drainage, Rio De Janiero, Vol. 1-F, International Commission on Irrigation and Drainage (ICID) G43.1–43.27.

Polyak, I. 1996 *Computational Statistics in Climatology*. Oxford University Press, Oxford.

Prasad, R., Deo, R. C., Li, Y. & Maraseni, T. 2018 Soil moisture forecasting by a hybrid machine learning technique: ELM integrated with ensemble empirical mode decomposition. *Geoderma* **330**, 136–161.

PWA 2011 *The Comparative Study of Options for an Additional Supply of Water for the Gaza Strip (CSO-G), the Updated Final Report*. Palestinian Water Authority.

PWA 2012 Palestinian water sector: status summary report. In *Preparation for the Meeting of the Ad Hoc Liaison Committee (AHLC)*, 23 September 2012. Palestinian Water Authority, New York.

PWA 2013 *National Water and Wastewater Policy and Strategy for Palestine: Toward Building A Palestinian State From Water Perspective*. Palestinian Water Authority.

PWA 2014 *Gaza Strip: No Clean Drinking Water, no Enough Energy, and Threatened Future*. Palestinian Water Authority.

PWA 2015 *Gaza Strip: Desalination Facility Project: Necessity, Politics and Energy*. Palestinian Water Authority.

Qahman, K. & Larabi, A. 2006 Evaluation and numerical modeling of seawater intrusion in the Gaza aquifer (Palestine). *Hydrogeology Journal* **14** (5), 713–728. doi:10.1007/s10040-005-003-2.

Rezaeianzadeh, M., Stein, A. & Cox, J. P. 2016 Drought forecasting using Markov Chain Model and artificial neural networks. *Water Resources Management* **30**, 2245–2259.

Saha, A., Ghosh, S., Sahana, A. S. & Rao, E. P. 2014 Failure of CMIP5 climate models in simulating post-1950 decreasing trend of Indian monsoon. *Geophysical Research Letters* **41**, 7323–7330. doi:10.1002/2014GL061573.

Sakizadeh, M., Mohamed, M. M. A. & Klammler, H. 2019 Trend analysis and spatial prediction of groundwater levels using time series forecasting and a novel spatio-temporal method. *Water Resources Management* **33**, 1425–1437. https://doi.org/10.1007/s11269-019-02208-9.

Samkhtin, V. U. & Hughes, D. A. 2004 Review Automated Estimation and Analyses of Drought Indices in South Asia. Working Paper 83. International Water Management Institute, Colombo, Sri Lanka.

Sastri, A. S. R. A. S. 1993 Agricultural drought management strategies to alleviate impacts: examples from the arid and sub-humid regions of the Indian subcontinent. In: Drought Assessment, Management, and Planning: Theory and Case Studies. Natural Resource Management and Policy, Vol. 2 (D. A. Wilhite, ed.). Springer, Boston, MA.

Sen, B., Topcu, S., Türkes, M., Baha Sen, B. & Warner, J. F. 2012 Projecting climate change, drought conditions and crop productivity in Turkey. Climate Research 52, 175–191. doi: 10.3354/cr01074.

Sene, K. 2009 Hydrometeorology Forecasting and Applications. Springer, UK.

Serfozo, R. 2009 Basics of Applied Stochastic Processes, 1st edn. Springer, Berlin, p. 443.

Shafer, B. A. & Dezman, L. E. 1982 Development of a surface water supply index (SWSI) to assess the severity of drought conditions in snowpack runoff areas. In Proceedings of the Western Snow Conference. Colorado State University, Fort Collins, CO, pp. 164–175.

Shah, R., Bharadiya, N. & Manekar, V. 2015 Drought index computation using standardized precipitation index (SPI) method for Surat District, Gujarat. Aquatic Procedia 4, 1243–1249. doi.org/10.1016/j.aqpro.2015.02.162.

Shahid, S. & Behrawan, H. 2008 Drought risk assessment in the western part of Bangladesh. Natural Hazards 46 (3), 391–413. doi:10.1007/s11069-007-9191-5.

Shahin, M., Van Oorschot, H. J. L. & De Lange, S. J. 1993 . Statistical Analysis in Water Resources Engineering. A.A. Balkema, Rotterdam, The Netherlands. p. 394.

Sharifi, A., Pourmand, A., Canuel, E. A., Ferer-Tyler, E., Peterson, L. C., Aichner, B. & Swart, P. K. 2015 Abrupt climate variability since the last deglaciation based on a high-resolution, multi-proxy peat record from NW Iran: The hand that rocked the Cradle of Civilization? Quaternary Science Reviews 123, 215–230.

Sharma, P., Machiwal, D. & Jha, M. K. 2019 Overview, current status, and future prospect of stochastic time series modeling in subsurface hydrology. GIS and Geostatistical Techniques for Groundwater Science 133–151. doi:10.1016/b978-0-12-815413-7.00010-9.

Sheffield, J. & Wood, E. F. 2011 Drought Past Problems and Future Scenarios, 1st Edition. Routledge, London.

Sheffield, J., Wood, F. E., Chaney, N., Guan, K., Sadri, S., Yuan, X., Olang, L., Amani, A., Ali, A., Demuth, S. & Ogallo, L. 2014 A drought monitoring and forecasting system for sub-Sahara African water resources and food security. Bulletin of the American Meteorological Society 95 (6), 861–882. doi:10. 1175/BAMS-D-12-00124.1.

Shukla, S. & Wood, A. W. 2008 Use of a standardized runoff index for characterizing hydrologic drought. Geophysical Research Letters 35 (2), 1–7. doi:10.1029/2007gl032487.

Sönmez, F. K., Kömüscü, A. Ü., Erkan, A. & Turgu, E. 2005 An analysis of spatial and temporal dimension of drought vulnerability in Turkey using the standardized precipitation index. Natural Hazards 35 (2), 243–264. doi:10.1007/s11069-004-5704-7.

Stagge, J. H., Tallaksen, L. M., Gudmundsson, L., Van Loon, A. F. & Stahl, K. 2015 Candidate distributions for climatological drought indices (SPI and SPEI). International Journal of Climatology 35 (13), 4027–4040. doi:10.1002/joc.4267.

Strazzo, S., Collins, D. C., Schepen, A., Wang, Q. J., Becker, E. & Jia, L. 2019 Application of a hybrid statistical–dynamical system to seasonal prediction of North American temperature and precipitation. Monthly Weather Review 147 (2), 607–625. doi:10.1175/mwr-d-18-0156.1.

Szalai, S. & Szinell, C. 2000 Comparison of two drought indices for drought monitoring in Hungary – a case study. Advances in Natural and Technological Hazards Research 161–166. doi:10.1007/978-94-015-9472-1_12.

Takafuji, E. H. d. M., Rocha, M. M. d. & Manzione, R. L. 2018 Groundwater level prediction/Forecasting and assessment of uncertainty using SGS and ARIMA models: a case study in the Bauru Aquifer System (Brazil). Natural Resources Research. doi:10.1007/s11053-018-9403-6.

Tefera, A. S., Ayoade, J. O. & Bello, N. J. 2019 Comparative analyses of SPI and SPEI as drought assessment tools in Tigray Region, Northern Ethiopia. SN Applied Sciences 1 (10). doi:10.1007/s42452-019-1326-2.

Thom, H. C. S. 1958 A note on the gamma distribution. Monthly Weather Review 86, 117–122.

Tirivarombo, S., Osupile, D. & Eliasson, P. 2018 Drought monitoring and analysis: standardized precipitation evapotranspiration index (SPEI) and standardized precipitation index (SPI). Physics and Chemistry of the Earth, Parts A/B/C. doi:10.1016/j.pce.2018.07.001.

Tong, H. 1990 Nonlinear Time Series: A Dynamical System Approach. Oxford University Press, Oxford.

Tsakiris, G., Pangalou, D. & Vangelis, H. 2007 Regional drought assessment based on the reconnaissance drought index (RDI). Water Resources Management 21 (5), 821–833. doi:10. 1007/s11269-006-9105-4.

Uddin, M. J., Hu, J., Islam, A. R. M. T., Eibek, K. U. & Nasrin, Z. M. 2020 A comprehensive statistical assessment of drought indices to monitor drought status in Bangladesh. Arabian Journal of Geosciences 13 (9). doi:10.1007/s12517-020-05302-0.

van der Geest, K., De Sherbinin, A., Kienberger, S., Zommers, Z., Sitati, A., Roberts, E. & James, R. 2019 The impacts of climate change on ecosystem services and resulting losses and damages to people and society. In: Loss and Damage From Climate Change. Climate Risk Management, Policy and Governance (R. Mechler, L. Bouwer, T. Schinko, S. Surminski & J. Linnerooth-Bayer, eds). Springer, Cham.

Vicente-Serrano, S. M., Beguería, S. & López-Moreno, J. I. 2010 A multiscalar drought index sensitive to global warming: the standardized precipitation evapotranspiration index.

Journal of Climate 23 (7), 1696–1718. doi:10.1175/2009jcli2909.1.

Werick, W. J. & Whipple, W. 1994 Managing Water for Drought. U.S. Army Corps of Engineers, Water Resources Support Center, Institute for Water Resource.

White, G. F. & Haas, J. E. 1975 Assessment of Research on Natural Hazards. MIT Press, Cambridge, MA.

Wichitarapongsakun, P., Sarin, C., Klomjek, P. & Chuenchooklin, S. 2016 Rainfall prediction and meteorological drought analysis in the Sakae Krang River basin of Thailand. Agriculture and Natural Resources 50 (6), 490–498. doi:10.1016/j.anres.2016.05.003.

World Meteorological Organization (WMO) & Global Water Partnership (GWP) 2016 Handbook of Drought Indicators and Indices (M. Svoboda and B.A. Fuchs). Integrated Drought Management Programme (IDMP), Integrated Drought Management Tools and Guidelines Series 2, Geneva

WSTF 2011 Indicators for water scarcity assessment. In Work in Progress Based on Meetings 13–26 May 2011, Ramallah, Palestine.

Xie, Z., Huete, A., Restrepo-Coupe, N., Ma, X., Devadas, R. & Caprarelli, G. 2016 Spatial partitioning and temporal evolution of Australia's total water storage under extreme hydroclimatic impacts. Remote Sensing of Environment 183, 43–52. doi:10.1016/j.rse.2016.05.017.

Xu, L., Chen, N., Zhang, X. & Chen, Z. 2018 An evaluation of statistical, NMME and hybrid models for drought prediction in China. Journal of Hydrology 566, 235–249.

Yeh, H.-F. & Hsu, H.-L. 2019 Stochastic model for drought forecasting in the Southern Taiwan Basin. Water 11 (10), 2041. doi:10.3390/w11102041.

Yuan, X. & Wood, E. F. 2013 Multimodel seasonal forecasting of global drought onset. Geophysical Research Letters 40 (18), 4900–4905. doi:10.1002/grl.50949.

Zaineldeen, U., Qahman, K. & Al-Dasht, J. 2013 Geological structure of the coastal aquifer in the southern part of the Gaza Strip, Palestine. Arabian Journal of Geosciences 7 (10), 4343–4354. doi:10.1007/s12517-013-1082-3.

Zhang, Q., Gemmer, M. & Chen, J. 2008 Climate changes and flood/drought risk in the Yangtze Delta, China, during the past millennium'. Quaternary International 176–177 (2008), 62–69. https://doi.org/10.1016/j.quaint.2006.11.004.

Zhang, D., Liu, X. & Bai, P. 2019 Assessment of hydrological drought and its recovery time for eight tributaries of the Yangtze River (China) based on downscaled GRACE data. Journal of Hydrology 568, 592–603.

Zhang, L., Wang, Y., Chen, Y., Bai, Y. & Zhang, Q. 2020 Drought risk assessment in Central Asia using a probabilistic copula function approach. Water 12, 421. doi:10.3390/w12020421.